

**DEVELOPMENT OF THIN FILM COMPOSITE  
NANOFILTRATION MEMBRANES WITH LAYER BY  
LAYER POLYELECTROLYTE DEPOSITION**

**A Thesis Submitted to  
the Graduate School of Engineering and Sciences of  
İzmir Institute of Technology  
in Partial Fulfillment of the Requirements for the Degree of**

**MASTER OF SCIENCE**

**in Chemical Engineering**

**by  
Önder TEKİNALP**

**July 2017  
İZMİR**

We approve the thesis of **Önder TEKİNALP**

**Examining Committee Members:**

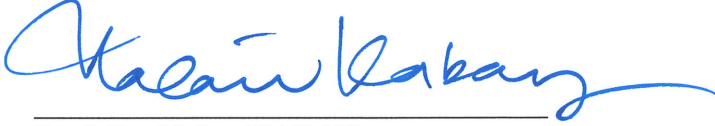
**Prof. Dr. Sacide ALSOY ALTINKAYA**

Department of Chemical Engineering, İzmir Institute of Technology



**Prof. Dr. Erol ŞEKER**

Department of Chemical Engineering, İzmir Institute of Technology



**Prof. Dr. Nalan KABAY**

Department of Chemical Engineering, Ege University

17 July 2017

**Prof. Dr. Sacide ALSOY ALTINKAYA**

Supervisor, Department of Chemical  
Engineering  
İzmir Institute of Technology



**Prof. Dr. Fehime ÇAKICIOĞLU ÖZKAN**  
Head of the Department of Chemical  
Engineering

**Prof. Dr. Aysun SOFUOĞLU**  
Dean of the Graduate School of  
Engineering and Sciences

## ACKNOWLEDGEMENTS

I would like to express my special thanks for those who contributed this thesis to be possible and not to refrain their supports during the lifetime of thesis. Working with my advisor Prof. Dr. Sacide Alsoy ALTINKAYA was a great privilege thanks to her continuous supervision, invaluable advises, significant concern and great patient. It has been a great honor to work with her to show the way how to be an honest and productive researcher. I would like to express my deepest appreciate to her to be eager for teaching and putting me into scientific field.

I would like to also thank to my committee members, Prof. Dr. Erol ŞEKER and Prof. Dr. Nalan KABAY for their valuable suggestions and recommendations to improve the quality of my thesis.

I would like to thank for my close friend and co-worker Canbike BAR for her supports, helps and being a sister in my life. My great thanks also my co-workers Aydın CİHANOĞLU and Nagehan ÇAĞLAR for their help and support both in the laboratory and daily life whenever I needed and made me think in another way. I feel great luck to know about them!

I would like to also thank to valuable people in Centre for Material Research for their kind help for SEM and AFM analyses and to provide an opportunity to use instruments any time I needed.

Finally, and most importantly, my gratefulness for my family; Ayşe SEZGİNCİ, Uğur SEZGİNCİ and Nil SEZGİNCİ for their moral support, motivation and encouragement during my lifetime. Without them this thesis would not exist!

## ABSTRACT

### DEVELOPMENT OF THIN FILM COMPOSITE NANOFILTRATION MEMBRANES WITH LAYER BY LAYER POLYELECTROLYTE DEPOSITION

Nanofiltration (NF) membranes are usually prepared in thin film composite (TFC) structure through polymerization of various monomers or coating of previously synthesized polymer on porous support membranes. Layer by layer (LbL) deposition of polyelectrolytes on a porous support is a facile and convenient method for the sake of producing NF membranes.

This study intends to manufacture TFC NF membrane via alternating polyelectrolyte deposition with limited number of layers on polysulfone/sulfonated polyethersulfone (PSF/SPES) porous support membrane. Polyethyleneimine (PEI) and alginate (ALG) were chosen as polyelectrolyte pairs. The support membranes with different pore sizes were prepared via nonsolvent induced phase inversion method by changing compositions and thickness of casting solution as well as composition of coagulation bath. The polyelectrolytes were deposited dynamically in a dead end filtration module at 1 bar. The influences of supporting electrolyte, polyelectrolyte pH and concentration as well as type of coating method on the membrane performances were investigated. The membranes were characterized by SEM, AFM, staining, and contact angle measurements. Stability and fouling tendency of produced membranes were determined. It was demonstrated that NF membrane (83% PEG1000 rejection) with a high flux ( $14 \text{ L/m}^2\cdot\text{h}\cdot\text{bar}$ ) can be manufactured by depositing only a single layer of PEI. Further deposition of ALG on PEI-coated membrane resulted in water permeability of  $15.5\pm 0.3 \text{ L/m}^2\cdot\text{h}\cdot\text{bar}$  with  $89.1\pm 0.6\%$  PEG1000 rejection by adjusting PSF:SPES ratio to 4:1.

# ÖZET

## KATMAN KATMAN POLİELEKTROLİT KAPLAMAYLA İNCE FİLM KOMPOZİT NANOFİLTRASYON MEMBRANLARININ GELİŞTİRİLMESİ

Nanofiltrasyon membranları genellikle ince film kompozit (TFC) yapıları şeklinde çeşitli monomerlerin polimerleşmeleri ya da önceden sentezlenmiş polimerin, destek membranlarının üzerine kaplanmasıyla hazırlanır. Polielektrolitlerin gözenekli bir destek üzerine tabaka tabaka kaplanması, nanofiltrasyon membranları üretebilmek için kolay ve elverişli bir yöntemdir.

Bu çalışma, gözenekli polisulfon/sülfonlanmış polietersülfon (PSF/SPES) destek membranı üzerine, sınırlı katman sayısı ve birbirini izleyen polielektrolit kaplama yöntemiyle TFC nanofiltrasyon membranı üretmeyi amaçlamıştır. Polietilenimin (PEI) ve alginat, polielektrolit çiftleri olarak seçildi. Çeşitli gözenek büyüklüklerine sahip destek membranları, döküm çözeltisinin bileşimi ve kalınlığının yanı sıra, koagülasyon banyosun bileşimini değiştirerek faz değiştirme yöntemiyle hazırlandı. Polielektrolitler, 1 bar'da sonlu filtre ünitesinde dinamik bir şekilde kaplandı. Kaplama yönteminin yanı sıra, polielektrolit pH ve konsantrasyonu ile destekleyici elektrolitin membran performansı üzerindeki etkileri incelendi. Membranlar taramalı elektron mikroskobu (SEM), atomik güç mikroskobu (AFM), boyama ve kontak açılı yöntemleriyle karakterize edildi. Üretilen membranların stabilite ve kirlenme eğilimi belirlendi. Sadece tek katman PEI ile kaplayarak, yüksek akıya sahip (14 L/m<sup>2</sup>.h.bar) nanofiltrasyon membranının (83 % PEG1000 tutma) üretilebileceği gösterildi. PSF:SPES oranını 4:1'e ayarlayarak ve PEI ile kaplanmış membran üzerine alginat katmanını ilave ederek saf su geçirgenliği 15.5±0.3 L/m<sup>2</sup>.h.bar olan ve PEG1000 geçişini 89.1±0.6 % engelleyen membran üretilmiştir.

# TABLE OF CONTENTS

LIST OF FIGURES .....	ix
LIST OF TABLES .....	xii
CHAPTER 1. INTRODUCTION .....	1
CHAPTER 2. LITERATURE REVIEW .....	4
2.1. Membrane Separation Process .....	4
2.2. Driving Forces of Membrane Separation Processes .....	5
2.3. Nanofiltration Process .....	6
2.4. Thin Film Composite (TFC) Membrane .....	7
2.5. LbL Self-Assembly .....	10
2.6. Deposition Parameters and Their Effects .....	11
2.6.1. Effect of pH .....	11
2.6.2. Effect of Supporting Electrolyte Concentration .....	12
2.6.3. Effect of Number of Layers .....	14
2.6.4. Effect of Coating Type .....	15
2.6.5. Effect of Molecular Weight of Polyelectrolyte .....	16
2.6.6. Effect of Polyelectrolyte Concentration .....	16
2.6.7. Effect of Polyelectrolyte Type .....	18
2.6.7.1. Polyethyleneimine (PEI) as a Cationic Polyelectrolyte .....	19
2.6.7.2. Alginate (ALG) as an Anionic Polyelectrolyte .....	20
2.7. Fouling .....	21
2.8. Stability .....	23
CHAPTER 3. MATERIALS AND METHODS .....	24
3.1. Materials .....	24
3.2. Membrane Preparation .....	24
3.2.1. Support Membrane Preparation via Phase Inversion .....	24
3.2.2. TFC Membrane Fabrication via Layer by Layer Assembly .....	25
3.3. Filtration Experiments .....	26

3.3.1. Water Flux Measurement.....	26
3.3.2. Rejection Measurement .....	27
3.3.3. Fouling Measurement .....	27
3.4. Surface Characterization.....	28
3.4.1. Staining .....	28
3.4.2. Scanning Electron Microscopy (SEM).....	28
3.4.3. Atomic Force Microscopy (AFM).....	28
3.4.4. Contact Angle .....	28
3.5. Stability.....	29
CHAPTER 4. RESULTS AND DISCUSSION.....	30
4.1. Optimization of Preparation Conditions for the Support Layer.....	30
4.1.1. Effect of Coagulation Bath Composition.....	31
4.1.2. Effect of Polymer Concentration .....	32
4.1.3. Effect of PSF:SPES Ratio.....	33
4.1.4. Effect of Thickness .....	34
4.1.5. Effect of Solvent Type .....	35
4.2. Optimization of Coating Conditions.....	38
4.2.1. Optimization of Coating Conditions on Support Prepared with PSF:SPES Ratio 5:1 .....	38
4.2.1.1. Effect of pH.....	38
4.2.1.2. Effect of Supporting Electrolyte .....	43
4.2.1.3. Effect of Coating Type (Dynamic versus Static).....	48
4.2.1.4. Effect of Polyelectrolyte Concentration.....	49
4.2.2. Optimization of Coating Conditions on Support Prepared with PSF:SPES Ratio 4:1 .....	50
4.2.2.1. Effect of pH.....	50
4.2.2.2. Effect of Ionic Strength in ALG Layer.....	52
4.3. Fouling Tendency and Stability of the Membranes.....	54
4.3.1. Antifouling property of LbL coated membrane.....	54
4.3.2. Stability of LbL coated layers.....	55

CHAPTER 5. CONCLUSION .....	56
REFERENCES .....	57



## LIST OF FIGURES

<b><u>Figure</u></b>	<b><u>Page</u></b>
Figure 2.1. Schematic representation of membrane separating two phases. ....	4
Figure 2.2. Classification of pressure driven based membrane processes. ....	6
Figure 2.3. NF membrane. ....	7
Figure 2.4. TFC membrane structure. ....	8
Figure 2.5. Schematic representation of a membrane preparation process by phase inversion technique. ....	8
Figure 2.6. Ternary phase diagram of polymer, solvent and nonsolvent. ....	9
Figure 2.7. LbL assembly by (a) dip, (b) spray and (c) spin coating. ....	11
Figure 2.8. Effect of pH on the conformation of adsorbed polyelectrolyte chains. ....	12
Figure 2.9. Effect of supporting electrolyte concentration on multilayer thickness. ....	13
Figure 2.10. Effect of ionic strength on membrane performance. ....	14
Figure 2.11. Effect of number of layer on rejection and flux. ....	14
Figure 2.12. Effect of LbL preparation method on the membrane a) Na <sub>2</sub> SO <sub>4</sub> rejections b) Na <sub>2</sub> SO <sub>4</sub> flux. ....	15
Figure 2.13. Effect of molecular weight of PEI a) 25000 Da b) 800 Da. ....	16
Figure 2.14. Effect of polyelectrolyte concentration on multilayer thickness. ....	17
Figure 2.15. Effect of CHI concentration on the membrane performance. ....	17
Figure 2.16. Effect of pH on PEI protonation degree and hydrodynamic radius. ....	20
Figure 2.17. Zeta potential of ALG as a function of pH. ....	21
Figure 3.1. LbL deposition by dynamic coating. ....	25
Figure 3.2. Dead-end filtration unit. ....	26
Figure 4.1. Effect of coagulation bath composition on the membrane performance. ....	31
Figure 4.2. Effect of polymer concentration on the membrane performance. ....	33
Figure 4.3. Effect of PSF:SPES ratio on membrane performance. ....	34
Figure 4.4. Effect of membrane thickness on membrane performance. ....	35
Figure 4.5. Effect of solvent type on membrane performance. ....	36
Figure 4.6. SEM images of the support membrane cast with 25 % polymer concentration (PSF:SPES blending ratio of 5) and 250 micron thickness. a) cross section, magnification 1000x b) cross section magnification 10000x c) surface magnification 100000x. ....	37

Figure 4.7. The effect of pH of PEI solution in the presence of 0.5 M NaCl on the membrane performance.....	39
Figure 4.8. Intensity of PEI-deposited membranes at pH 3 and pH 7 in the presence of 0.5 M NaCl. ....	39
Figure 4.9. AFM images of membranes deposited at a) pH=3 and b) pH=7 in the presence of 0.5 M NaCl. ....	41
Figure 4.10. PEI layer adsorption at pH 4, 6 and 9. ....	42
Figure 4.11. The effect of pH of PEI solution during PEI (0.5 M NaCl)/ALG (0 M NaCl) deposition on the membrane performance. ....	43
Figure 4.12. The effect of adding NaCl into PEI solution (pH=7) on the membrane performance. ....	44
Figure 4.13. The effect of adding NaCl into PEI solution (pH=3) on the membrane performance. ....	44
Figure 4.14. Intensity of PEI-deposited membranes in the absence and presence of 0.5 M NaCl at pH 7.....	45
Figure 4.15. AFM images of the coated membranes.....	46
Figure 4.16. Surface SEM images of a) bare support and pH 7 PEI-coated membranes in the presence of b) 0 M NaCl c) 0.5 M NaCl.....	47
Figure 4.17. The effect of coating type on the membrane performance. NaCl concentrations in PEI (pH=7)/ALG (pH=7) solutions are 0.5 M and 0 M, respectively. ....	49
Figure 4.18. The effect of polyelectrolyte concentration on the membrane performance. NaCl concentrations in PEI (pH=7)/ALG (pH=7) solutions are 0.5 M and 0 M, respectively. ....	50
Figure 4.19. The effect of pH of PEI solution during PEI/ALG deposition on the membrane performance. ....	51
Figure 4.20. Contact angle measurement of support with PSF:SPES ratio a) 4:1 and b) 5:1 ....	51
Figure 4.21. The effect of salt addition in ALG solution during PEI/ALG deposition on the membrane performance.....	52
Figure 4.22. SEM images of the support membrane cast with 25% polymer concentration (PSF:SPES blending ratio of 4) and 250 micron thickness a) cross section magnification 1000x b) surface magnification, 100000x. ....	53

Figure 4.23. Fouling tendency of the produced NF membrane and commercial polyethersulfone membrane in dead-end filtration module.....	54
Figure 4.24. Stability measurement of PEI/ALG coated membrane. ....	55

## LIST OF TABLES

<b><u>Table</u></b>	<b><u>Page</u></b>
Table 2.1. Membrane separation processes and corresponding driving forces. ....	5
Table 2.2. Common Foulants Used in NF/RO Membranes in Various Processes. ....	22
Table 4.1. Casting conditions of the membrane A and B. ....	31
Table 4.2. Casting conditions of the membrane B and C. ....	32
Table 4.3. Casting conditions of the membrane C and D. ....	33
Table 4.4. Casting conditions of the membrane D and E. ....	34
Table 4.5. Casting conditions of the membrane E and F. ....	35
Table 4.6. Effect of pH on degree of protonation and Stokes-Einstein radius of 7200 Da PEI. ....	40
Table 4.7. Fouling resistances of membranes. ....	55

# CHAPTER 1

## INTRODUCTION

NF is a pressure-driven membrane separation process that is considered to be energy efficient as well as environment-friendly. Its characteristics extends between reverse osmosis (RO) and ultrafiltration (UF); therefore, it offers higher permeability than RO. It requires relatively low operating pressure and lower costs as compared to RO and offering better retention than ultrafiltration. The molecular weight cut off of a NF membrane lies between 100–1000 Da indicating NF membranes have a maximum pore diameter of approximately 2 nm (Cheng et al., 2011). NF membrane separates molecules based on both size and Donnan exclusion and provides high selectivity for separating multivalent ions from monovalent ones. Therefore, it is used for water treatment process such as water softening and brackish water purification (Sanyal and Lee, 2014). The other applications of NF process are in oil industry, organic recovery, and food industry (Sun, 2015). In most applications, the use of membrane separation process is often restricted by fouling due to an accumulation of rejected material on the surface or within pores of the membrane leading to a decline in its performance, hence, more energy is required resulting in higher operating costs. Therefore, it is crucial to develop NF membranes tending to reduce fouling, having high stability and separation capabilities (Ba et al., 2010).

NF membranes are usually prepared in the form of a TFC structure. TFC membranes are composed of two distinct layers that are porous support and active layer. The porous layer is generally formed by phase inversion and the selective layer is formed by in-situ polymerization or surface coating (Pendergast and Hoek, 2011). Building strong interaction between support and active layer is vital for a long-term stability of the membranes during operation. In addition, the active selective layer should be as thin as possible to minimize mass transfer resistance for filtration. In order to overcome these two challenges, deposition of multilayer polyelectrolyte films in a LbL assembly is an attractive method for manufacturing TFC membranes. The thickness of deposited layers is usually on the order of a few nanometers and the strength of binding between the layers and support can be adjusted through controlling charge density of each layer since the driving force for depositing layers is generally

electrostatic interaction (Sanyal and Lee, 2014). Various deposition conditions such as ionic strength, pH, concentration of the polyelectrolyte solution, number of adsorbed layers, type of coating (dynamic or static), molecular weight and type of polyelectrolyte can be adjusted to control the selectivity and permeability of the constructed membranes (Sun, 2015). Several groups have utilized the LbL technique for preparing TFC NF membranes. Krasemann et al. (2001) demonstrated as many as 60 bilayers of oppositely charged PEI/polyvinylsulfate (PVS) and poly(allylamine hydrochloride) (PAH)/PVS polyelectrolytes deposition so as to obtain TFC membrane with a high selectivity. On the other hand, Lajimi et al. (2011) developed NF membrane by statically adsorbing 20 bilayers of ALG and chitosan (CHI) layers on cellulose acetate (CA) substrate. They demonstrated almost 100% of divalent salt retention and pure water permeability around 3 L/m<sup>2</sup>hbar. Malaisamy and Bruening (2005) reduced deposition cycle down to 7 layers of poly(styrenesulfonate) (PSS)/protonated poly(allylamine) (PAH) by restricting molecular weight cutoff of the support membrane to 50 kDa. They demonstrated 95% SO<sub>4</sub><sup>2-</sup> rejection 14.1 L/m<sup>2</sup>hbar pure water permeability and < 500 molecular weight cutoff (MWCO) value by adsorbing 3.5 bilayers of PSS/PAH statically. Recently, Rajabzadeh et al. (2014) prepared positively charged NF membrane by successive deposition of PSS/PAH polyelectrolytes on polyethersulfone support. They reported 12 L/m<sup>2</sup>hbar pure water permeability with 94% Mg<sup>2+</sup> rejection by statically coating two bilayers. Ba et al. (2014) manufactured positively charged NF membrane by first immersing the P84 copolyimide based support membrane into PEI solution and then dynamically coating this PEI modified membrane with negatively charged polyacrylic acid (PAA) or PVS or neutral polymer polyvinyl alcohol (PVA) through electrostatic interaction and hydrogen bonding, respectively. They reported highest permeability with PVA coating around 3 L/m<sup>2</sup>hbar with 85% of divalent Ca<sup>2+</sup> and almost 82% of raffinose rejection. Although only two layers were deposited to achieve 85% of Ca<sup>2+</sup> rejection, the permeability of the membrane is low that requires high operating pressure during filtration. The commercial flat sheet NF PES10 membrane involving an active layer of polyethersulfone with polyvinylpromidone as co-polymer on polypropylene carrier has a 1000 Da MWCO, a pure water permeability between 5-10 L/m<sup>2</sup>hbar and 40–70% Na<sub>2</sub>SO<sub>4</sub> rejection (Wang and Chung, 2005).

The objective of this thesis is to manufacture TFC NF membranes by means of LbL assembly of polyelectrolytes on PSF/SPES porous support membrane with only a

few layers. PEI and ALG were deposited dynamically at 1 bar in a dead end filtration module. The membranes were characterized by staining, AFM, SEM analyses, and contact angle measurement. In addition, stability and fouling tendency of the membranes were also investigated. TFC NF membrane was prepared by dynamic LbL deposition of merely one bilayer of PEI/ALG polyelectrolyte pair with  $15.5 \pm 0.2$  L/m<sup>2</sup>.h.bar of pure water permeability and  $89.1 \pm 0.6\%$  of PEG1000 rejection.

This thesis is composed of five chapters. Following Chapter 1, a literature review was shown in Chapter 2 to acquire an extensive understanding of the basics of NF process, LbL, polyelectrolyte-based TFC membranes as well as significant deposition parameters. Materials used and the details of experimental studies performed during the thesis were given in Chapter 3. In Chapter 4, results were discussed and finally in Chapter 5, general conclusions from the studies conducted in this thesis were summarized.

## CHAPTER 2

### LITERATURE REVIEW

#### 2.1. Membrane Separation Process

A membrane is a selective barrier between two phases. It allows passage of some molecules, ions or particles through its porous structure so that it facilitates separation of substances (Mulder, 1997). Schematic representation of membrane separation process is shown in Figure 2.1. Main goal of research in membrane field is to produce highly selective membrane with a long-term sustainable permeability of flowing fluid passing through the membrane.

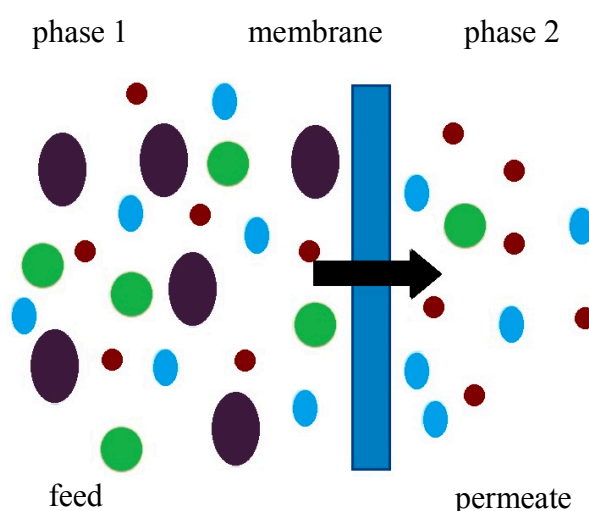


Figure 2.1. Schematic representation of membrane separating two phases.  
(Source: Reprinted with permission from Joseph et al. (2014))

Membrane separation processes have significant advantages as compared to conventional separation methods such as absorption, distillation or extraction. The application area of this separation process covers a wide range making this technology quite versatile in industry. Another important advantage of this process is its simplicity in scaling up which nominates membrane process competitive among other separation technologies. It is also possible to perform membrane separation process efficiently at low temperature that requires low energy resulting in saving in terms of cost (Ahmed, 2010). In addition, membrane processes are considered as nontoxic and environmentally friendly since no additives are required for separation (Mulder, 1997).



## 2.2. Driving Forces of Membrane Separation Processes

Main driving forces applied during membrane separation processes can be classified as electrical potential difference, concentration difference, temperature difference and pressure difference that are shown in Table 2.1 with the corresponding membrane separation processes utilizing these forces (Mulder, 1997).

Table 2.1. Membrane separation processes and corresponding driving forces.  
(Source: Adapted from Bachok (2012))

<b>Driving Force</b>	<b>Membrane Process</b>
Pressure Differences	Microfiltration (MF) Ultrafiltration (UF) Nanofiltration (NF) Reverse osmosis (RO)
Chemical Potential Differences	Pervaporation Dialysis Gas separation Liquid membranes
Electrical Potential Differences	Electrodialysis
Temperature Differences	Membrane distillation

Types of membrane processes in which pressure difference is used as a driving force can be classified as MF, UF, NF and RO. Figure 2.2 shows the range of pressures applied for each process and typical pore sizes in the corresponding membranes. Average pore size of the membrane decreases from MF down to RO membranes, consequently, pressure difference applied increases in this order in order to achieve reasonable flux values.

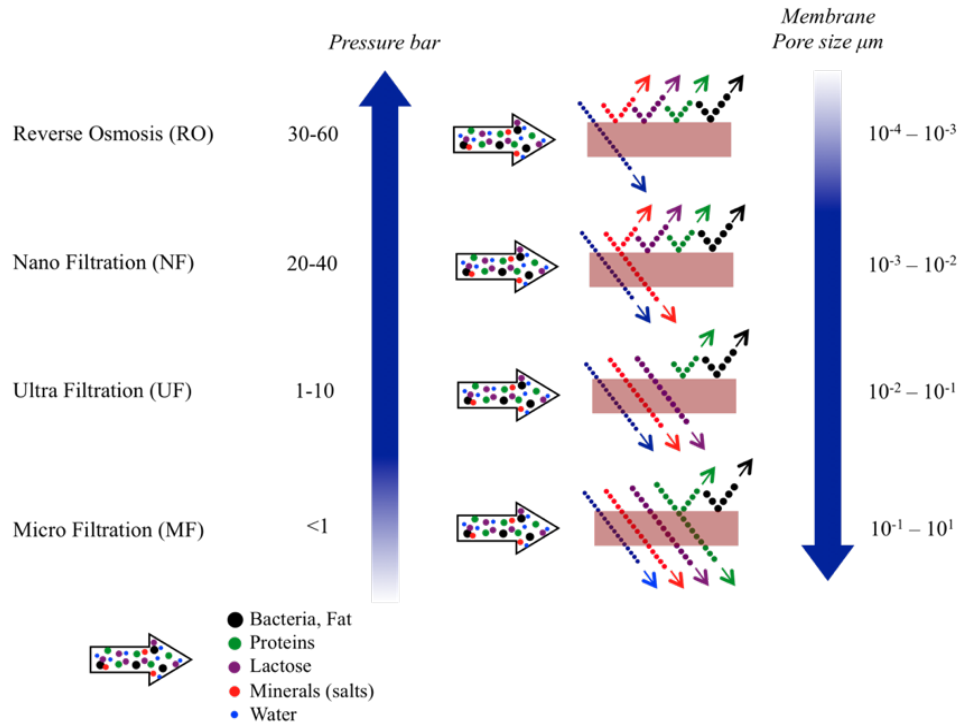


Figure 2.2. Classification of pressure driven based membrane processes.  
(Source: Taken from Wu and Imani (2012))

### 2.3. Nanofiltration Process

NF whose properties lies between UF and RO is a pressure-driven membrane filtration process requiring pressure less than 40 bar. It offers two distinct separation mechanism based on pore size and charged portions of the membrane. Being ideal for the rejection of multivalent ions, it facilitates selectivity of ions by size exclusion and Donnan exclusion. Typical pore size in NF membranes is within 1-5 nm corresponding to molecular weight cut-off (MWCO) of 200-1000 g/mole (Stanton et al., 2013; Ahmed, 2010). It is a less energy intensive process as compared to RO due to the larger pore size in NF membranes. Thereby, using NF as a pretreatment step for RO plants allows significant saving in energy costs. NF covers a wide range of applications like water softening, wastewater treatment, recovery of valuable compounds in biotechnology, pharmaceutical and textile industry (Wang et al, 2009). Typical schematic representation of a NF membrane was shown in Figure 2.3.

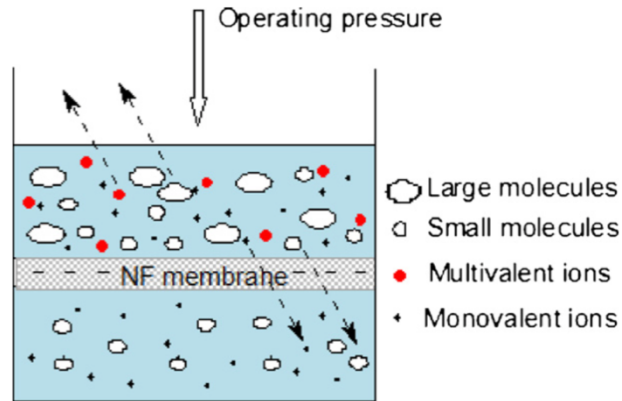


Figure 2.3. NF membrane.  
 (Source: Reprinted with permission from Zhao et al. (2011))

NF membranes can be produced by classical phase inversion technique in a single step or as a TFC structure with a two-step preparation protocol. The phase inversion method is the process of the transformation of polymer solution from a liquid phase into a solid phase. Even though single step preparation by phase inversion is a simple technique, it is not always easy to obtain desired pore size with all types of polymers. Therefore, this method is not competitive in the market in manufacturing NF membranes. On the other hand, in the case of TFC membranes, the properties of top and support layer can be adjusted independently that affords achieving better membrane performances (Rajesh et al., 2013).

## 2.4. Thin Film Composite (TFC) Membrane

For NF process, obtaining membrane with high retention and flux as well as being resistant to fouling for a given application is crucial which is related with the membrane structure and the surface properties. To satisfy these requirements, TFC membranes can be nominated. TFC membranes consist of two layers which are ultra-thin top layer serving as selective barrier and porous MF or UF sub-layer providing smooth surface for thin top layer to locate as shown in Figure 2.4. If it is desired, non-woven reinforcing fabric can be used to supply mechanical strength for composite membrane during high pressure application (Dalwani, 2011).

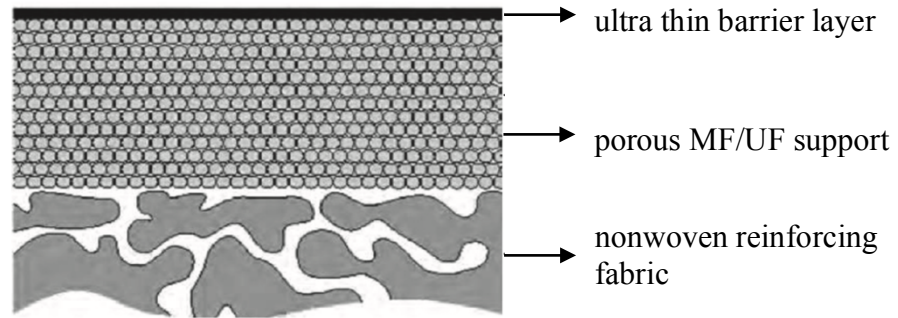


Figure 2.4. TFC membrane structure.  
(Source: Taken from Dalwani (2011))

The manufacturing of TFC membrane starts with the formation of porous support layer by means of phase inversion method. In this method, first homogeneous casting polymer solution prepared by dissolving polymer in a suitable solvent is placed into a coagulation bath involving non-solvent as represented in Figure 2.5. Depending on the casting conditions and the rate of exchange of solvent and nonsolvent, instantaneous or delayed precipitation occurs and polymer-rich and polymer-poor phases are formed. Once the exchange of solvent and nonsolvent is complete, and the membrane is dried, polymer-rich phase forms the matrix while polymer lean phase leads to porous structure (Ning, 2015).

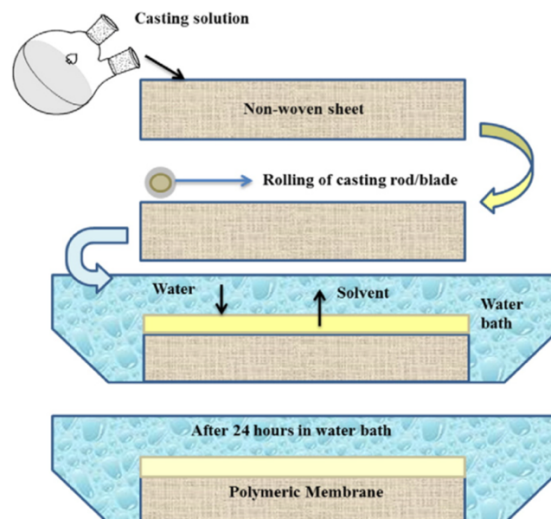


Figure 2.5. Schematic representation of a membrane preparation process by phase inversion technique. (Source: Reprinted with permission from Jhaveri et al. (2016))

To control membrane structure and morphology, equilibrium ternary phase diagram is used as a tool. In a ternary phase diagram, which involves polymer (P),

solvent (S) and nonsolvent (NS), homogeneous one phase region is separated from a heterogeneous two phase region by a binodal line (Ning, 2015).

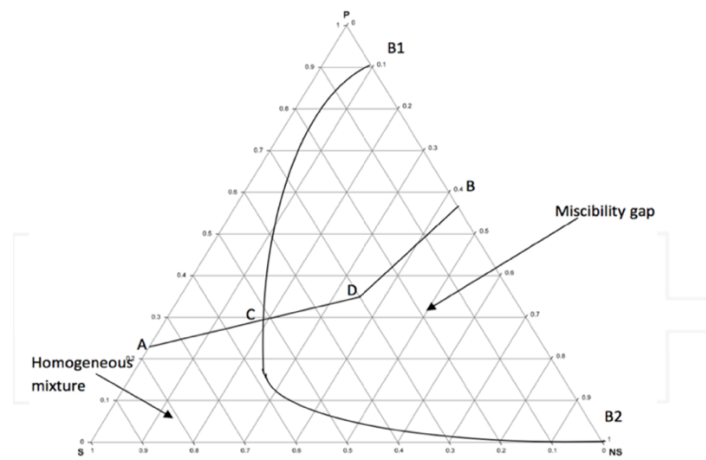


Figure 2.6. Ternary phase diagram of polymer, solvent and nonsolvent.  
(Source: Taken from Ning (2015))

Point A in Figure 2.6 corresponds to initial casting solution including polymer dissolved in solvent. Once point C is reached, phase separation occurs. Point C denotes that polymer-rich phase at the upper boundary and polymer-lean phase at the lower boundary of demixing gap are produced. At point D, polymer rich-phase is considered to be enough for solid formation and further diffusion of solvent and nonsolvent to the point B results in final membrane composition. Porosity of the membrane is determined at point B corresponding to solid-polymer rich phase. On the other hand, points B1 and B2 represent liquid solvent rich phase (Ning, 2015).

Mostly, UF membranes are used as the supporting layer in the manufacturing of TFC membranes due to their good solvent resistance, chemical and thermal stability. Generally, PSF, polyether sulfone (PES), polyacrylonitrile (PAN), polyetherimide (PEI) and polypropylene (PP) are used for preparing support membranes (Minhas et al., 2013). Most UF membranes have molecular weight cut-off (MWCO) values between 1,000 and 100,000 Da. However, in order to obtain TFC NF membrane with relatively low number of layers at desired performance, selection of support is quite critical in terms of its pore size and charge density. Malaisamy and Bruening (2005) indicated that MWCO of the support should not be higher than 50 kDa to convert UF support membrane to a NF membrane with a limited number of layers. They developed NF membrane by depositing 3.5 bilayers PSS/PDADMAC onto PES support membrane having 50 kDa MWCO value.

Techniques for preparing TFC membrane can be divided into two main categories which are in-situ polymerization involving plasma polymerization, grafting and interfacial polymerization and the surface coating also corresponding to the LbL assembly on a support layer (Dalwani, 2011). In in-situ polymerization techniques, complicated and harsh pretreatments are required which restricts their application. In addition, during interfacial polymerization, physically adhesion of active layer on the support is formed and leads to serious performance damage and a sharp decrease in lifetime of TFC membranes. Therefore, it is quite crucial to construct a robust interfacial adhesion between active layer and support layer (Li et al., 2015). To deal with those obstacles, LbL for TFC membrane preparation is proposed by Decher and Hong (Burke and Barrett, 2004).

## **2.5. LbL Self-Assembly**

LbL sequential coating of polyelectrolytes on a porous surface is a charming technique for manufacturing selective and ultrathin membrane by means of electrostatic, hydrogen bonding or covalent bonding (Sanyal and Lee, 2014). The LbL technique provides mechanically stable films due to the strong electrostatic interactions between charged units. In addition, defect free thin films without pinholes in nanometer-scale can be manufactured conditions. Being simple, economical and environmentally friendly technique, LbL method has widespread applications including controlled drug delivery, molecular sensors, artificial muscles, solid battery electrolytes, and separation membranes (Wang et al., 2009).

The polyelectrolyte deposition in a LbL manner can be achieved using spin coating, spray coating and dip coating as shown in Figure 2.7. During spray and spin coating fast deposition is possible, however, huge amount of polyelectrolyte loss is experienced and spin coating is merely applicable for small areas (Michel et al., 2012). Dip-coating is an efficient process involving successive immersion of the substrate into oppositely charged polyelectrolyte solutions for a certain time, followed by a rinsing step. In general, multilayers prepared by dip-coating are thicker, denser and smoother as compared to those prepared via spray coating under similar conditions (Joseph et al., 2014).

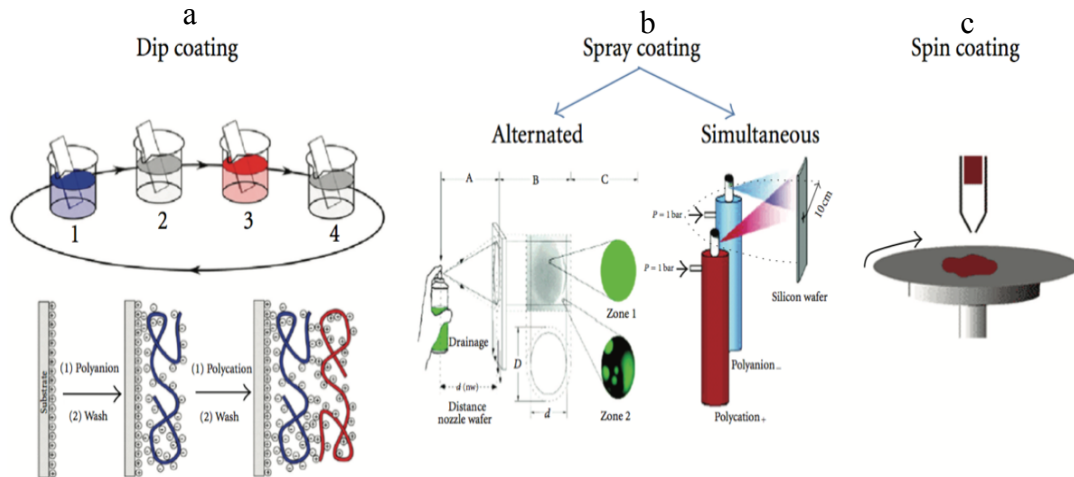


Figure 2.7. LbL by (a) dip, (b) spray and (c) spin coating.  
(Source: Taken from Michel et al. (2012))

## 2.6. Deposition Parameters and Their Effects

One of the most important privilege in LbL method is that it is easy to tune the surface properties so as to obtain high selective and high flux membrane by influencing the interaction strength between support-polyelectrolytes and polyelectrolytes itself. To achieve better performances, deposition conditions are adjustable which are pH of polyelectrolytes, supporting electrolyte concentration, number of layers, type of coating, polyelectrolyte molecular weight (MW) and concentration as well as polyelectrolyte type which have an effect on the membrane structure, properties and stability (Joseph et al., 2014).

### 2.6.1. Effect of pH

pH is an indispensable parameter in order to adjust charge density of weak polyelectrolytes affecting film thickness along with permeability and morphology. Since, the ionization groups in weak polyelectrolytes can be adjusted by changing pH of solution (Joseph et al., 2014).

Sanyal (2016) modified NF 90 commercial membrane with 5-bilayers of PAH and PAA at pH of 8.5 and 3.5, respectively as well as both at pH 6.5. They demonstrated that the lowest film thickness was obtained at pH 6.5 since both polyelectrolytes are fully charged at this pH that offered a thin flat film deposition via strong electrostatic interaction which was shown in Figure 2.8. On the other hand, thick

and loopy structure was displayed at a pH of 8.5 and 3.5 for PAH and PAA respectively owing to the partially charged configuration. They reported higher permeability and rejection for a system deposited at a pH 6.5 due to lower thickness of the polyelectrolyte layers and higher ionic cross linking density providing smaller pore sizes.

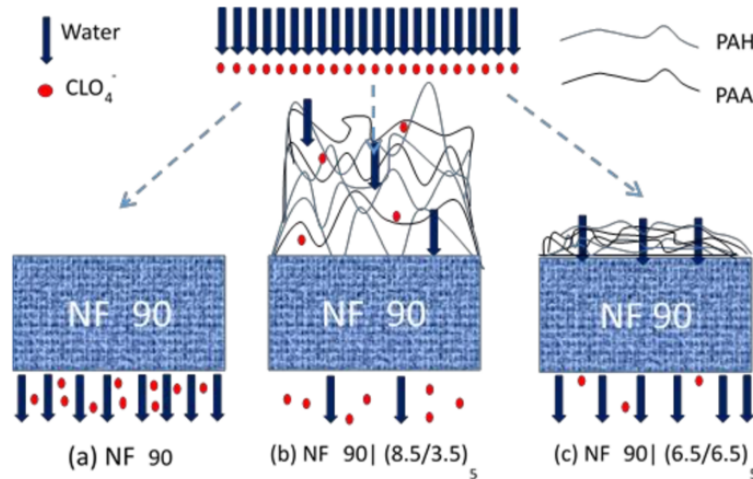


Figure 2.8. Effect of pH on the conformation of adsorbed polyelectrolyte chains. (Source: Taken from Sanyal (2016))

Ouyang et al. (2008) investigated the effect of pH of positively weak (PAH) and negatively strong (PSS) polyelectrolytes on the membrane performance. Since PAH is a weak polyelectrolyte, they changed its charge density by changing solution pH from 2.3 to 4.5. They observed lower  $Mg^{2+}$  rejection at pH 4.5 due to carrying less charge at this pH resulting in lower degree of ionic cross linking than at pH 2.3. On the other hand, due to being strong polyelectrolyte, the degree of protonation of PSS remained same when its pH was changed from 2.1 to 2.3, hence, no significant performance change was observed.

## 2.6.2. Effect of Supporting Electrolyte Concentration

Supporting electrolyte concentration of the polyelectrolyte solution has a significant effect on interaction between polyelectrolyte layers and charged support layer. It is pointed out the added salts could either increase or decrease the adsorption of polyelectrolytes depending on the repulsion between the polyelectrolyte segments and attraction between polyelectrolyte segments and the substrate surface. Salt screens both



the segment–segment repulsion within polyelectrolytes increasing the adsorption of polyelectrolytes, and the segment–surface attraction between polyelectrolytes and the substrate surface decreasing the adsorption of polyelectrolytes (Wang et al., 2009).

By increasing salt concentration in polyelectrolyte solution, thicker and more coiled structures are obtained due to the charge screening of polyelectrolyte chain inhibiting electrostatic interaction between layers (Joseph et al., 2014). Effect of supporting electrolyte concentration on multilayer thickness was represented in Figure 2.9.

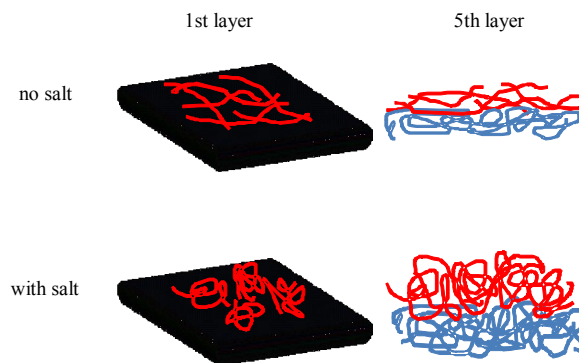


Figure 2.9. Effect of supporting electrolyte concentration on multilayer thickness.  
(Source: Taken from Adusumilli (2010))

Stanton et al. (2003) studied the effect of salt concentration with 4.5 bilayers films terminated in a PSS layer ([PSS/PAH]<sub>4</sub>PSS). They observed decrement in water flux with an increment in salt concentration presumably due to increased osmotic pressure. On the other hand, they increased Na<sub>2</sub>SO<sub>4</sub> salt rejection up to 95% by increasing supporting electrolyte concentration owing to higher surface charge during deposition of the last layer of PSS. They explained that film thickness was increased with a more loop structure due to the screening effect of high concentration salt on charged groups of polymers.

Wang et al. (2009) studied sPEEK and PEI layers on the PAN substrate and they observed decrease in salt rejection and increased in flux when the concentration of NaCl in the polyelectrolyte solution was increased as shown in Figure 2.10. This was ascribed to the formation of looser layers allowing passage of molecules easier at high ionic strength.

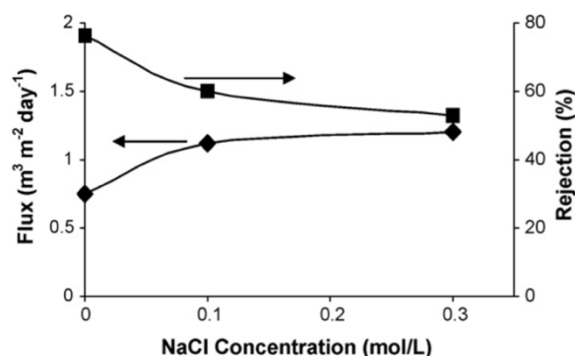


Figure 2.10. Effect of ionic strength on membrane performance. (Source: Reprinted with permission Wang et al. (2009))

### 2.6.3. Effect of Number of Layers

Number of deposited layers is another significant parameter for the membrane performance. As it is expected, higher the number of layers coated, better the surface coverage.

Wang et al. (2009) observed that as the number of layers of sPEEK and PEI onto the PAN support was increased rejection characteristic of the membranes was improved while water flux decreased as represented in Figure 2.11.

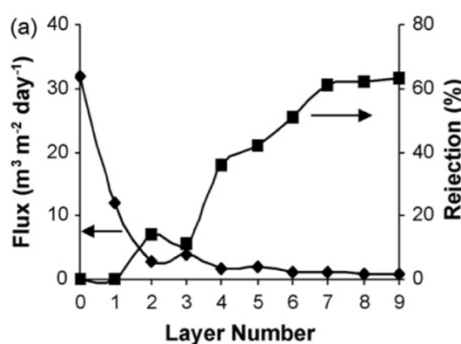


Figure 2.11. Effect of number of layer on rejection and flux. (Source: Reprinted with permission Wang et al. (2009))

Ouyang et al. (2008) improved flux around 40 % by decreasing number of layers from [PSS/PAH]4 to [PSS/PAH]3. However, they observed decrease in  $Mg^{+2}$  rejection significantly due to the lack of surface coverage.

Qin et al. (2013) prepared NF membrane for the removal of divalent metal ions by adsorbing PSS and PEI on a PAN ultrafiltration support. They showed that increasing number of layers resulted in higher  $Ni^{+2}$  and  $Cd^{+2}$  rejection due to better surface coverage.

## 2.6.4. Effect of Coating Type

Coating of polyelectrolytes on support membranes can be carried out dynamically or statically. In dynamic coating, polyelectrolyte solution is forced towards the membrane surface. Dynamic coating might propose a better selection in the deposition process as compared to static coating in which adsorption of polyelectrolytes diffuses to the surface without any applied force. It is anticipated to offer better membrane performance owing to the better polyelectrolyte distribution on support (Ng et al., 2013).

Su et al. (2012) compared static and dynamic coating of PDADMAC/PSS layers in terms of permeability and rejection of the membrane as shown in Figure 2.12.

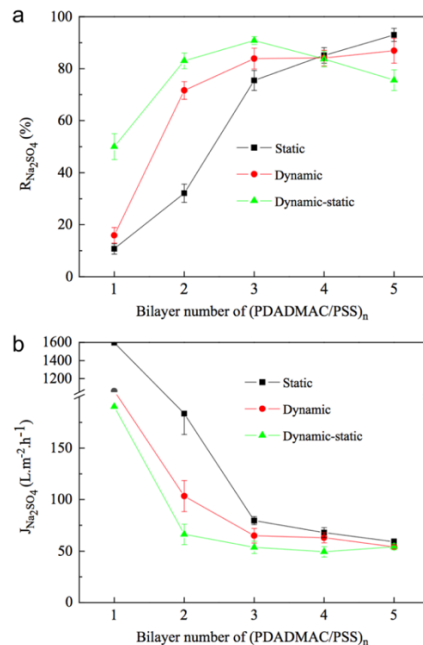


Figure 2.12. Effect of LbL preparation method on the membrane a) Na<sub>2</sub>SO<sub>4</sub> rejections  
b) Na<sub>2</sub>SO<sub>4</sub> flux. (Source: Reprinted with permission Su et al. (2012))

As seen from the figure 2.12, when relatively low number of polyelectrolytes was deposited, significant salt rejection difference in favor of dynamic coating was obtained. For two layers coating, 30%, 70% and 85% of rejection was measured via static, dynamic and static-dynamic coating, respectively. This result indicated that coating in a dynamic manner can reduce the number of layers substantially to achieve the same membrane performance (Su et al., 2012).

### 2.6.5. Effect of Molecular Weight of Polyelectrolyte

Effect of the molecular weight of the polyelectrolytes is significant for the membrane performance. Bridging capability of the polyelectrolytes varies with the magnitude of the molecular weight due its chain length.

Wang et al. (2009) studied the effect of molecular weight (MW) of PEI on the membrane performance as represented in Figure 2.13. They prepared NF membrane by statically depositing PEI and sPEEK via LbL method on PAN support. They demonstrated better salt rejection with lower number of layers for high molecular weight PEI. In contrary, they stated that to observe significant salt rejection, higher number of bilayers were required for low MW PEI. Besides, for single layer, significant difference was observed between flux of the membranes prepared with high and low MW PEI. They deduced that chain length of the low MW PEI caused a looser structure and worse bridging capability owing to chain length resulting in higher flux and lower rejection.

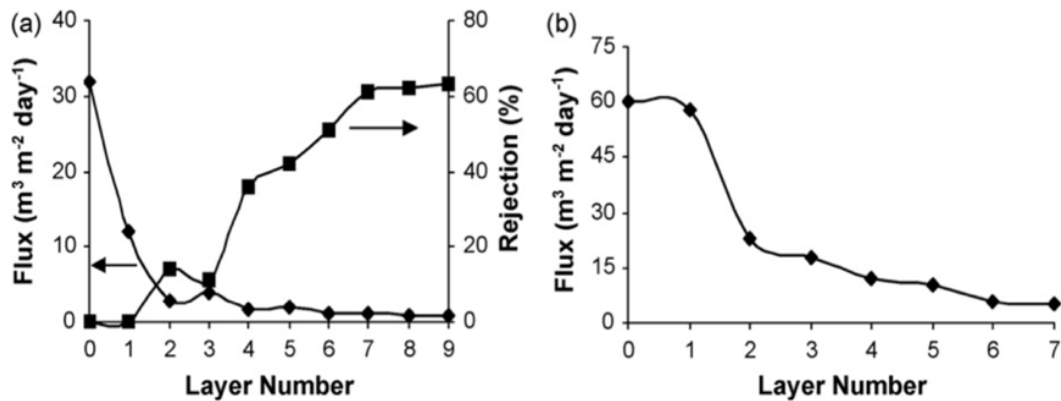


Figure 2.13. Effect of molecular weight of PEI a) 25000 Da b) 800 Da. (Source: Reprinted with permission Wang et al. (2009))

### 2.6.6. Effect of Polyelectrolyte Concentration

Effect of polyelectrolyte concentration is another indicator to control surface thickness in LbL method for obtaining better membrane performance. A general correlation between polymer concentration and thickness of the films is represented in Figure 2.14.

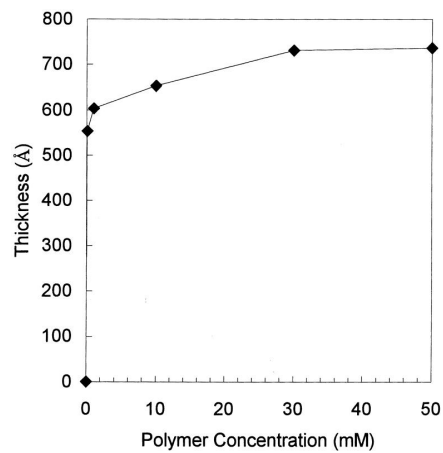


Figure 2.14. Effect of polyelectrolyte concentration on multilayer thickness. (Source: Reprinted with permission Adusumilli (2010))

Xu et al. (2011) investigated the effect of chitosan (CHI) concentration in the range of 1-5 g/L as shown in Figure 2.15. With the increased chitosan concentration, the salt rejection was improved from 91% to 95% while flux slightly decreased.

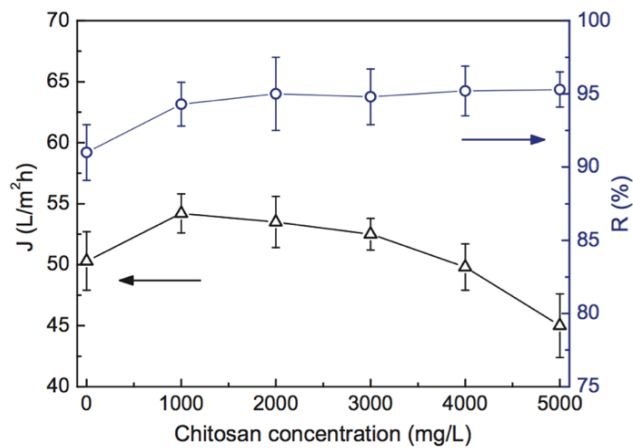


Figure 2.15. Effect of CHI concentration on the membrane performance. (Source: Reprinted with permission Xu et al. (2011))

They ascribed salt rejection improvement to the formation of thicker and more compact layer of CHI on the surface of membrane.

Yun et al. (2014) studied the effect of PEI concentration on the surface morphology of PEI films deposited onto SiO<sub>2</sub> substrate. Increment in PEI concentration lead to increase in thickness and decrease in surface roughness due to fully cover of PEI film with a flat surface.

### 2.6.7. Effect of Polyelectrolyte Type

Polyelectrolyte type can specify the membrane properties such as thickness, roughness, porosity, hydrophilicity and swellability dramatically due to mostly their structure being weak or strong polyelectrolyte and amount of charge they carry. Therefore, selection of polyelectrolyte pairs is quite crucial in order to obtain NF membrane with desired pore size. Common polyelectrolyte pairs used in preparing NF membranes are CHI/ALG (Lajimi et al., 2011), PEI/PSS (Qin et al., (2013; Liu et al., 2010), PSS/PDADMAC (Malaisamy and Bruening, 2005), PAA/PEI (Rajabzadeh et al., 2014) and PAA/PAH, PAH/PSS (Ouyang et al., 2008).

Fu et al., (2009) demonstrated different growth mechanism for alternating deposition of PEI and PAA at different pH. By alternating pH of two deposited polyelectrolytes, degree of ionization, hence, amount of adsorbed mass was controlled due to the change in charge density and diffusivity of weak polyelectrolytes. When PEI and PAA multilayer was deposited at a pH of 8 and 5 respectively, nonlinear increase in thickness and mass was observed that lead to a dramatic increase in roughness. On the other hand, smoothness of the surface was controlled by adjusting the pH of polyelectrolytes to 7 for both which enabled a linear increase in thickness and mass owing to the change in degree of ionization. Therefore, it is crucial working with weak polyelectrolytes so as to obtain desired membrane performance by adjusting their ionization degree during deposition due to being pH responsive.

In the study, PEI and ALG were chosen as weak polyelectrolytes. PEI carries high charge density in its structure and it has ability of high solvent, thermal and flame resistance (Sun, 2015). On the other hand, ALG has a low toxicity and is biodegradable as well as carrying negative charge in a wide pH range (Zhou et al., 2013). Both PEI and ALG are weak polyelectrolytes and their charge density can be adjusted by pH which influences how PEI chains adsorb onto a surface, which in turn affects the overall properties of the membranes. On the other hand, multilayer films prepared from strong polyelectrolytes do not represent pH-responsive behavior and remain fully charged over the entire pH range (Burke and Barrett, 2004).

### **2.6.7.1. Polyethyleneimine (PEI) as a Cationic Polyelectrolyte**

PEI is a cationic weak polyelectrolyte which allows the complexation with anionic materials. Two types of PEI exist which are branched PEI containing primary, secondary and tertiary amino groups and linear PEI involving all secondary amines in its structure. Both types of PEI are favorable as cationic polyelectrolytes thanks to their solvent and high thermal resistance (Sun, 2015). Because of being a polycation, decreasing PEI solution pH leads to the protonation of amine groups which is a crucial parameter for surface modification during LbL assembly (Lindquist and Stratton, 1976). pH dependency of PEI is shown in Figure 2.16 where black data points represents charged PEI monomers and white data points denotes uncharged monomers. In the basic region corresponding to pH values between 9.5-12, aggregation of PEI is dominant and has a zeta potential of near zero at pH 11. In the neutral region denoting pH values between 6.8-9.5, hydrodynamic diameter of PEI increases as a result of decrease in aggregation and the degree of protonation increases to 44% and stays constant over this range. In weak acidic region between pH 4 and 6.8 significant protonation increment is observed around 70% and hydrodynamic radii of the polymer increases due to the intra-chain repulsion of segments. In strong acidic region that corresponds to the pH value between 2 and 4, not significant increase in protonation degree is observed and below pH 3, protonation degree reaches to 95%. On the other hand, hydrodynamic diameter of PEI decreases most probably due to the repulsion between highly charged polyions. Beyond pH 2, buffering does not exist due to maximum protonation of PEI segments (Curtis et al., 2016).

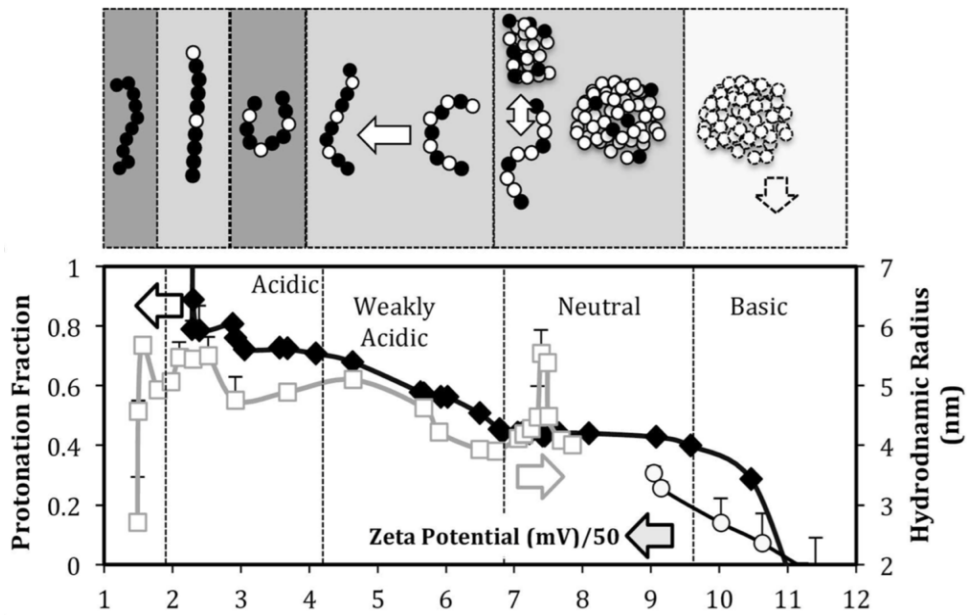


Figure 2.16. Effect of pH on PEI protonation degree and hydrodynamic radius. (Source: Taken from Curtis et al. (2016))

Wang et al. (2009) deposited PEI onto the negatively charged PAN substrate to improve salt rejection and fouling properties. They demonstrated relatively high salt rejection around 89 % with only 3.5 bilayer of branched PEI and sulfonated poly (ether ether ketone) (sPEEK).

In the study of Liu et al. (2010), PEI terminated films resulted in higher binding capacity relative to the PAH or PDADMAC for the produced membrane.

### 2.6.7.2. Alginate (ALG) as an Anionic Polyelectrolyte

ALG is a polysaccharide with a homogenous charge distribution and it is extracted from the cell walls of brown sea-weed. This semi-flexible linear block copolymer accounts for 1,4-linked  $\beta$ -D-mannuronic acid and  $\alpha$ -L-guluronic acid residues. ALG charge density can be easily tuned by pH, since it is weak polyelectrolyte and it is negatively charged at any pH as shown below in Figure 2.17 (Loosli et al., 2014).



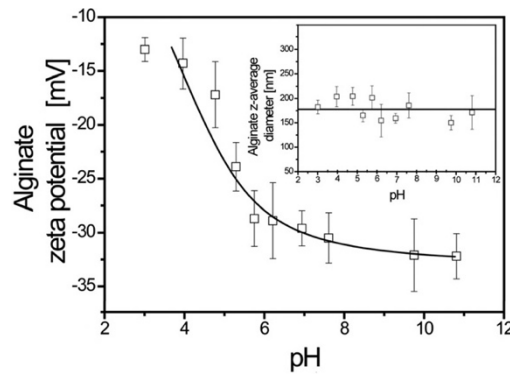


Figure 2.17. Zeta potential of ALG as a function of pH.  
(Source: Reprinted with permission from Loosli et al. (2014))

Lajimi et al. (2011) studied LbL deposition of ALG by making use of its negative charge with cationic polyelectrolyte chitosan for surface modification of cellulose acetate membranes. They obtained NF membrane by deposition of 15-20 bilayers of ALG/CHI polyelectrolytes.

## 2.7. Fouling

In membrane filtration processes, membrane lifetime and performances measured in terms of permeability and selectivity are influenced by the accumulation of particles, colloids, macromolecules, salts or biomolecules like bacteria on the membrane surface and within the membrane pores. This phenomenon is called as membrane fouling due to the effects of adsorption, cake layer deposition or concentration polarization (Escobar and Bruggen, 2015). Fouling mechanisms can be mainly categorized as:

- **pore constriction:** partially rejected matter is adsorbed within the membrane pores,
- **cake formation:** completely rejected matter gathers on top of the membrane surface,
- **pore blocking:** pore is plugged by particles due to the similarity in size.

Physical interaction and chemical degradation between the membrane surface and the foulants such as inorganic, organic, and biological substances result in fouling phenomena in many different forms. Accumulation of organic and colloidal foulants form cake layers and bio-fouling is inevitable when membrane surface is exposed to bacterial colonies (Escobar and Bruggen, 2015).

Membrane surface characteristics play key role to affect fouling. These major factors can be listed as surface roughness, charge and hydrophobicity of the membranes. In order to reduce costs related with fouling control, it is important to control membrane surface properties (Hobbs et al., 2006). The types of foulants and their control mechanism for NF/RO systems are given in the Table 2.2 (Schäfer et al. (2004)).

Table 2.2. Common Foulants Used in NF/RO Membranes in Various Processes.  
(Source: Adapted from Schäfer et al. (2004))

<b>Foulants</b>	<b>Control Method</b>
General	Hydrodynamics/shear Operation below critical flux Chemical cleaning
Inorganic	Acid addition Pre-treatment Additives (antiscalants)
Organic	Pre-treatment using biological processes Activated carbon Ion exchange Enhanced coagulation
Colloids (<0.5 $\mu\text{m}$ )	Pre-treatment using coagulation & filtration Microfiltration Ultrafiltration
Biological Solids	Pre-treatment using disinfection (e.g. chlorination) Filtration Coagulation Microfiltration Ultrafiltration

Ba et al. (2014) used PVA, PVS and PAA polymers to increase membrane fouling resistance. They obtained NF membranes with antifouling property by making use of hydrophilicity of these polymers. The surface charge of the PVS and PAA coated membranes was almost zero and fouling due to the charge-charge interaction was decreased.

Wang et al. (2009) prepared neutrally charged NF membrane by assembly of negatively charged SPEEK onto a positively charged surface. Fouling tendency of the

membranes decreased as a result of hydrophilic and neutral character of the SPEEK modified surface.

## **2.8. Stability**

Even though NF membranes assembled by LbL has significant advantages among conventional produced NF membranes, poor stability of oppositely charged polyelectrolytes by electrostatic interaction could be faced under the harsh conditions such as high ionic strength over long-term use. This drawback is required to deal with so as to produce LbL-assembled NF membranes with improved stability under high ionic strength (Fadhillah et al., 2013).

## CHAPTER 3

### MATERIALS AND METHODS

#### 3.1. Materials

PSF and SPES were used in the fabrication of porous support membrane. PSF with a molecular weight of 35 kDa was purchased from Sigma Aldrich and SPES with a molecular weight of 80 kDa was kindly denoted by Konishi Chemicals, Japan. Solvents, 1-methyl-2-pyrrolidone (NMP) and N,N-Dimethylacetamide (DMAc) with a purity of >99.5% and >99% used to dissolve PSF and SPES were purchased from Fluka and Sigma Aldrich, respectively. PEI (MW=750 kDa) and Alginate sodium salt from brown algae (Alginate, MW=80-120 kDa) used to manufacture TFC membrane were supplied from Sigma Aldrich. Sodium hydroxide (NaOH), sodium chloride (NaCl) and hydrochloric acid (HCl) with 37% purity used to adjust degree of ionization of polyelectrolytes and ionic strength of the polyelectrolyte solution were purchased from Sigma Aldrich and Merck, respectively. Polyethylene glycol (MW=1000 Da) purchased from Aldrich was used to perform rejection tests of the membranes. In order to investigate charge alteration owing to deposition of charged polyelectrolytes, Congo Red bought from Aldrich were used. Albumine from bovine serum (BSA, MW=66 kDa) used to measure fouling tendency of produced membranes was purchased from Sigma Aldrich.

#### 3.2. Membrane Preparation

##### 3.2.1. Support Membrane Preparation via Phase Inversion

PSF and SPES polymers were used to prepare support membranes via nonsolvent induced phase inversion method. Before preparing polymer solution, polymers were dried overnight at 80°C. Dried polymers with different compositions were dissolved in NMP or NMP: DMAc solvent mixture with 150 rpm stirring for 24 h. After complete dissolution, polymer solution was waited for another 24 h to get rid of possible bubbles formed during stirring. Then, part of the polymer solution was poured onto clean defect free flat glass plate and a casting knife was rolled along the polymer

solution by varying distance between the knife and the plate from 250  $\mu\text{m}$  to 300  $\mu\text{m}$  at room temperature. Casting procedure was followed by dipping polymer solution into the coagulation bath including deionized water or water and NMP mixture at 4°C and room temperature. Polymers are not soluble in coagulation bath, on the other hand, exchange of solvent in the polymer solution and nonsolvent in the bath results in phase inversion. After waiting for 10-minute in coagulation bath, membrane formed was rinsed with clean DI water and stored in refrigerator until further use to prevent possible microbial growth within membrane structure. Membranes were stored in water for at least 24 h before testing to ensure removal of all solvent from the structure.

### 3.2.2. TFC Membrane Fabrication via Layer by Layer Assembly

After fabricating porous support membrane via phase inversion, TFC membrane preparation was started by depositing positively charged PEI solution on negatively charged PSF/SPES support in a dead end filtration unit (Millipore, Amicon Stirred Cell 8010) at 1 bar for 10 min as shown in Figure 3.1. PEI solution was prepared at desired concentration and its pH was adjusted by 0.1-1 M HCl and 0.1-0.5 M NaOH solutions. After coating of PEI, membrane surface was rinsed with almost 200 ml DI water in order to remove weakly adsorbed polyelectrolyte. After rinsing, the DI water was permeated through the membrane at 2.5 bar until steady state is reached. Afterwards, PEI-coated membrane was exposed to negatively charged ALG and rinsing procedure and then compaction of membrane at 2 bar were followed as described above. Deposition of ALG on the PEI layer was achieved under dynamic and static conditions. In dynamic coating 1 mL of ALG was filtered through the membrane at 1 bar.

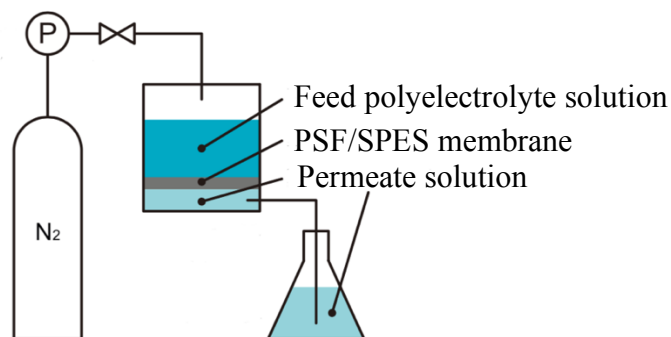


Figure 3.1. LbL deposition by dynamic coating.  
(Source: Reprinted with permission from Saeki et al. (2013))

### 3.3. Filtration Experiments

#### 3.3.1. Water Flux Measurement

Dead-end cell filtration module with 10 ml volume (Millipore 8010) was used to test permeability and rejection properties of the membranes. The membrane with a surface area of 4.1 cm<sup>2</sup> was left on a rigid sponge and placed in the cell. The cell was fitted with a pressure gauge as shown in Figure 3.2. Transmembrane pressure difference through the membrane was generated with pressurized nitrogen gas. The feed solution was stirred at 300 rpm. Each membrane was initially pressurized at 2.5 bar for compaction to reach a steady state flux. Then the pressure was lowed to the operating pressure of 2 bar. Amount permeated through the membrane was recorded as a function of time until all liquid in the cell was filtered and the flux  $J_w$  (L/m<sup>2</sup>h) and the pure water permeability (PWP) of the membranes were calculated by the following equations:

$$J_w = \left( \frac{\Delta V}{A \times \Delta t} \right)$$

$$\text{PWP} = \left( \frac{\Delta V}{A \times \Delta t \times \Delta P} \right)$$

where  $\Delta V$  is the volume of permeated water (L),  $A$  (m<sup>2</sup>) is the membrane area,  $\Delta t$  (h) is the permeation time and  $\Delta P$  (bar) is the transmembrane pressure difference applied through the membrane. The experiments were carried out at room temperature.

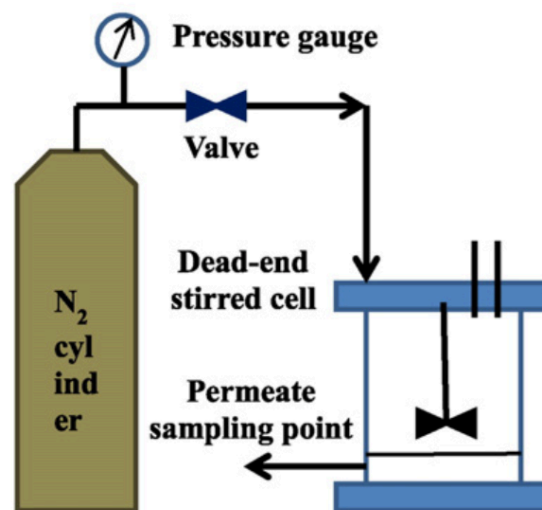


Figure 3.2. Dead-end filtration unit.  
(Source: Reprinted with permission from Jhaveri and Murthy (2016))

### 3.3.2. Rejection Measurement

Polyethylene glycol (PEG) with a molecular weight of 1000 was dissolved in DI water to prepare 1 g/L of concentration and rejection measurements were carried out using a dead-end filtration unit.

10 ml of PEG 1000 solution was filtered at 2 bar until 5 ml of permeate was collected. The concentrations of PEG 1000 in the feed ( $C_f$ ), permeate ( $C_p$ ) and in the retentate ( $C_r$ ) were determined using Rudolph - J357 Automatic Refractometer. The rejection was then calculated as follows:

$$R (\%) = \left( 1 - \frac{C_p}{\frac{C_f + C_r}{2}} \right) \times 100$$

### 3.3.3. Fouling Measurement

To determine fouling tendency of the membranes, first pure water permeability of the clean membranes ( $PWP_i$ ) was measured and then the stirred cell was refilled with BSA solution with 1 g/l concentration at pH= 7.0. The flux of BSA solution permeating through the membranes was measured at 2 bar for 15 h. After filtering BSA solution, the membranes were washed with distilled water. This was followed by water permeability measurement of cleaned membranes ( $PWP_c$ ). The flux recovery (FR) was calculated as follow:

$$FR (\%) = \left( \frac{PWP_c}{PWP_i} \right) \times 100$$

To analyze the fouling process in detail, the membrane resistance ( $R_m$ ), irreversible fouling resistance ( $R_{ir}$ ), total fouling resistance ( $R_t$ ) and reversible fouling resistance ( $R_r$ ) were calculated by following equations.

$$R_{\text{membrane}} = \left( \frac{1}{PWP_i} \right)$$

$$R_{ir} = \left( \frac{1}{PWP_c} - \frac{1}{PWP_i} \right)$$

$$R_t = \left( \frac{1}{\text{BSA solution permeability}} \right)$$

$$R_r = R_t - (R_{\text{membrane}} + R_{ir})$$

## **3.4. Surface Characterization**

### **3.4.1. Staining**

On account of polyelectrolyte adsorption, charge alteration was anticipated after each deposition. In order to investigate this behaviour, staining experiment was performed. PEI deposited membrane was immersed into a 1 g/L of negatively charged congo red (CR) solution prepared at pH 7 whose isoelectric point is at pH 3 (Yaneva and Georgieva, 2012). Membranes were kept in dye solutions for one hour. Afterwards, membranes were washed with water until water became colorless. Aventes-Avemouse62 spectrophotometer was used to determine the intensity of each color corresponding to amount of the charged groups on the membrane stained by CR.

### **3.4.2. Scanning Electron Microscopy (SEM)**

Cross section and surface topography images of the dried membranes were analyzed by scanning electron microscopy (SEM) via FEI Quanta 250 FEG instrument. Before analyzing with SEM, gold was used to coat dried samples via Magnetron Sputter Coating Instrument.

### **3.4.3. Atomic Force Microscopy (AFM)**

Atomic force microscopy (AFM) analysis was performed in air by using MMSPM Nanoscope 8 from Bruker. Scanning was performed in tapping mode for 5x5  $\mu\text{m}$  surface by using TAP150 model tip (material: 0.01-0.025 Ohm-cm Antimony (n) doped Si) for dried membranes.

### **3.4.4. Contact Angle**

Hydrophilicity of the membranes were determined by water drop contact angle measurement using Attension Optical tensiometer. Before measurement, membranes were dried to make sure it was free of humid. Afterwards, membranes were cut in a specific dimension and fixed on a glass slide. 4 measurements were performed for each membrane with 5  $\mu\text{l}$  volume of liquid droplet.



### **3.5. Stability**

The stability of the membrane after bilayer deposition was investigated by storing the membrane in 1 M NaCl solution under static conditions. The water permeability and PEG 1000 rejection of the membrane were measured at the end of 7 and 14 days of storage in NaCl solution.

## CHAPTER 4

### RESULTS AND DISCUSSION

In TFC NF membranes, the selectivity and rejection properties are mainly determined by the thin top layer. The main aim in this thesis is to develop NF membrane by depositing a single bilayer polyelectrolyte pair on the porous UF membrane. To achieve this task, first of all support membranes with suitable pore size and charge density were prepared by changing phase inversion conditions such as coagulation bath composition, polymer concentration in the casting solution, membrane thickness and polymer blend ratio (SPES:PSF). Optimization of preparation conditions for the support membrane plays a key role. This is due to the fact that if the molecular weight cut off value of the support membrane is large, then, it is unlikely to convert it into a NF membrane by a coating successive layers of polyelectrolytes. In the following sections, first the results on the optimization of preparation conditions for the porous support layer and then optimization of polyelectrolyte deposition conditions was given. In the final section, the results on the stability and organic fouling tendency of the selected membranes were reported.

#### **4.1. Optimization of Preparation Conditions for the Support Layer**

The support membrane was prepared by nonsolvent induced phase inversion technique. In order to change the rate of liquid-liquid and liquid-solid demixing, hence, to control the ultimate structure of the membranes, conditions in the casting solution (solvent type, polymer concentration, casting thickness and SPES:PSF ratio) and in the coagulation bath (coagulation bath composition) were changed. The best preparation conditions were selected based on the pure water flux and PEG 1000 rejection properties of the membranes coated with the PEI and ALG polyelectrolyte pair. In the following discussions, one bilayer coating corresponds to 2 successive layers of PEI/ALG and 1.5 bilayer means deposition of PEI/ALG/PEI layers.

#### 4.1.1. Effect of Coagulation Bath Composition

The coagulation bath composition influences the final membrane morphology. Water is commonly used as a nonsolvent but it can be mixed with additives basically to change the viscosity and the rate of precipitation. In this work, 2% NMP which corresponds to the same amount used for dissolving polymer was added into the nonsolvent water bath. Casting conditions of the membrane A and B are represented in Table 4.1.

Table 4.1. Casting conditions of the membrane A and B.

Membrane	PSF:SPES (wt:wt)	Polymer Concentration (wt%)	Membrane Thickness ( $\mu\text{m}$ )	Solvent	% Solvent in Nonsolvent Water Bath
A	5.7:1	20	300	NMP	2
B	5.7:1	20	300	NMP	-

The results in Figure 4.1 have represented membrane performance in the absence and presence of 2% NMP in coagulation bath (CB).

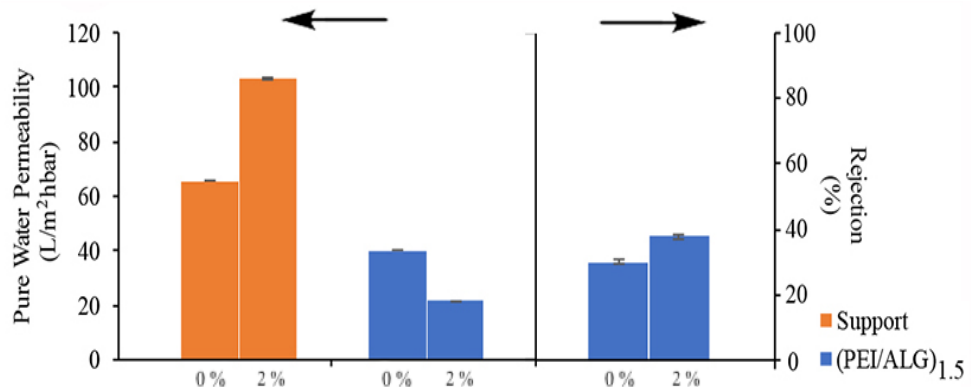


Figure 4.1. Effect of coagulation bath composition on the membrane performance.

By adding 2% NMP in the coagulation bath the pure water permeability of the support membrane increased by 58 %. This can be explained by decreased polymer concentration at the polymer solution/coagulation bath interface leading to a more open membrane structure (Guillen et al., 2011). It was noted that after 1.5 bilayer

PEI/ALG/PEI coating, the permeability of the support membrane casted in the presence of 2 % NMP in water decreased by a factor of almost 5 (79%) while the decrease was 39% for the membrane coagulated in pure water bath. This could be due to penetration of part of the polyelectrolytes into the more porous support membrane in the case of 2% NMP causing increased mass transfer resistance. On account of significant decrease in water permeability and only slight improvement in PEG 1000 rejection (with 2% NMP  $37.8 \pm 0.70$  and 0% NMP  $30.1 \pm 0.50\%$ ), it was decided not to add NMP into the coagulation bath.

#### 4.1.2. Effect of Polymer Concentration

The PEG1000 rejection values reported in Figure 4.1 (< 50 %) simply indicated that the pore size of the support membrane is large and three layers of polyelectrolyte deposition is not enough to reduce the surface pore size of the membrane to the level required for a NF membrane (< 2 nm). To reduce the pore size, the polymer concentration in the casting solution was increased from 20% to 25% as represented in Table 4.2.

Table 4.2. Casting conditions of membrane B and C.

Membrane	PSF:SPES (wt:wt)	Polymer Concentration (wt%)	Membrane Thickness ( $\mu\text{m}$ )	Solvent	% Solvent in Nonsolvent Water Bath
B	5.7:1	20	300	NMP	-
C	5.7:1	25	300	NMP	-

As shown in Figure 4.2, the increase in polymer content dramatically reduced pure water permeability from  $65.7 \pm 0.30$  L/m<sup>2</sup>hbar to  $19.2 \pm 0.40$  L/m<sup>2</sup>hbar. With the increased polymer concentration in the casting solution, a membrane with smaller pores and lower porosity is obtained as a result of higher polymer concentration at the coagulation bath interface during phase inversion (Mulder, 1997). Depositing one bilayer of PEI/ALG pair on the support membrane containing 25% polymer resulted in a NF rejecting 88% of PEG 1000 molecules.

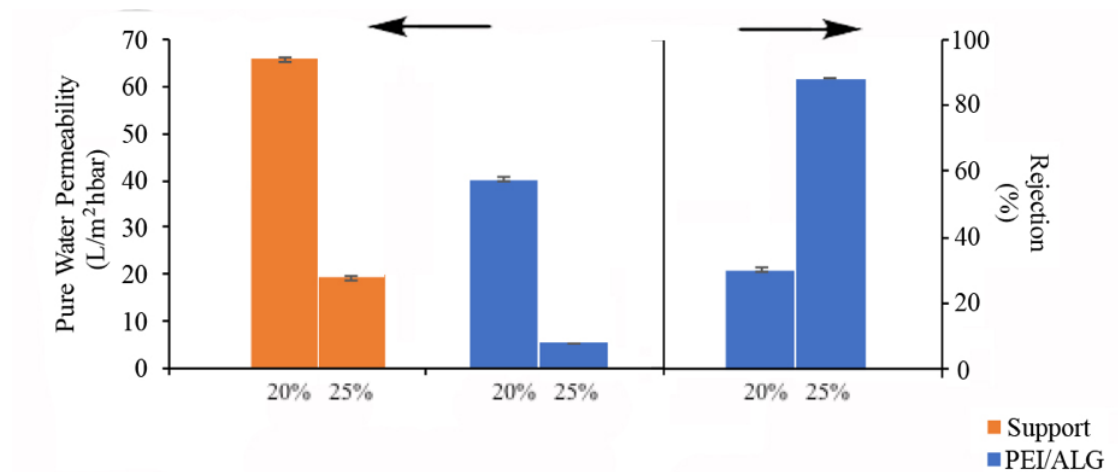


Figure 4.2. Effect of polymer concentration on the membrane performance.

#### 4.1.3. Effect of PSF:SPES Ratio

Even though the membrane prepared with 25% polymer and the PSF:SPES blending ratio of 5.7:1 is in the NF category, its permeability value was found low. Therefore, it was decided to increase the SPES content as represented in Table 4.3 since the water flux of the hydrophobic polymer PSF is enhanced in the presence of SPES (Jacob et al., 2014).

Table 4.3. Casting conditions of the membrane C and D.

Membrane	PSF:SPES (wt:wt)	Polymer Concentration (wt%)	Membrane Thickness ( $\mu\text{m}$ )	Solvent	% Solvent in Nonsolvent Water Bath
C	5.7:1	25	300	NMP	-
D	5:1	25	300	NMP	-

As seen from the results in Figure 4.3, increasing amount of SPES in the membrane composition lead to increment in the permeability of the support membrane. On the other hand, the differences in the permeability and PEG 1000 rejection values of the two membranes prepared with PSF:SPES ratios of 5.7 and 5 were found insignificant after one bilayer PES/ALG coating.

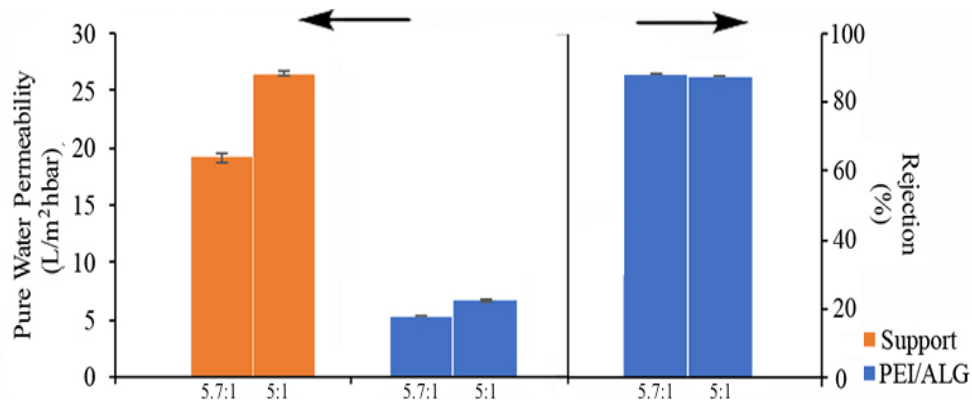


Figure 4.3. Effect of PSF:SPES ratio on membrane performance.

#### 4.1.4. Effect of Thickness

In order to increase the permeability of the membrane without losing its selectivity, the casting thickness was decreased from 300 to 250 micron as shown below in Table 4.4. The results have shown that the decrease in thickness did not improve the permeability of the support membrane on the other hand significant improvement in rejection was obtained after one bilayer PEI/ALG coating.

Table 4.4. Casting conditions of the membrane D and E.

Membrane	PSF:SPES (wt:wt)	Polymer Concentration (wt%)	Membrane Thickness (µm)	Solvent	% Solvent in Nonsolvent Water Bath
D	5:1	25	300	NMP	-
E	5:1	25	250	NMP	-

Lower PEG 1000 rejection by the membrane cast with 300 micron could be due to less SO<sub>3</sub>H groups on the surface, hence, less PEI adsorption by electrostatic attraction to the surface. In this case, fraction of the pores on the surface covered by the polyelectrolyte deposition becomes smaller compared to the case on the membrane cast with 250 micron. Based on the results shown in Figure 4.4, it was demonstrated that the membrane manufactured is in the NF category.

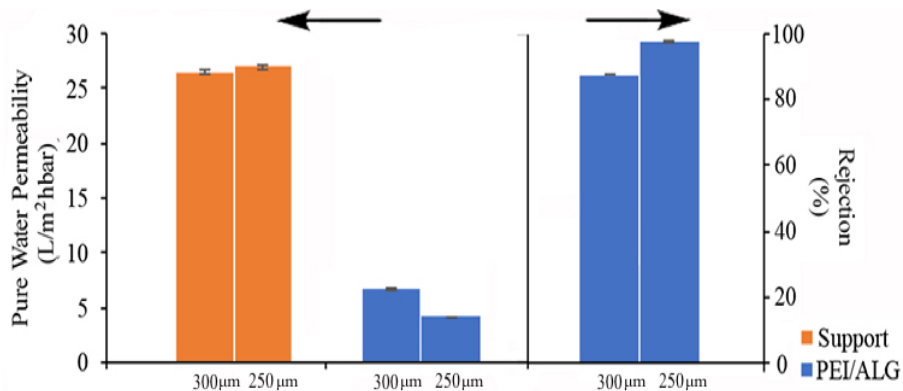


Figure 4.4. Effect of membrane thickness on membrane performance.

Hence, it was decided to continue casting the membranes with 25% polymer concentration (PSF:SPES blending ratio of 5) and 250 micron thickness and further parametric changes were tried for the sake of improving pure water permeability of the membranes.

#### 4.1.5. Effect of Solvent Type

Solvent type has a significant influence on membrane structure and performance. Solvent should be miscible with the nonsolvent and dissolve the polymer completely (Guillen et al. 2011).

Table 4.5. Casting conditions of the membrane E and F.

Membrane	PSF:SPES (wt:wt)	Polymer Conc. (wt%)	Membrane Thickness (μm)	Solvent	% Solvent in Nonsolvent Water Bath
E	5:1	25	250	NMP	-
F	5:1	25	250	DMAC:NMP (2:1)	-

To investigate the influence of adding another solvent into the solution, the membrane is cast with a mixture of DMAC and NMP (DMAC:NMP ratio 2:1) as shown in Table 4.5 and results were represented in Figure 4.5. It was seen that using DMAC and NMP mixture in the casting solution increased the permeability of the support membrane by a factor of almost 2.

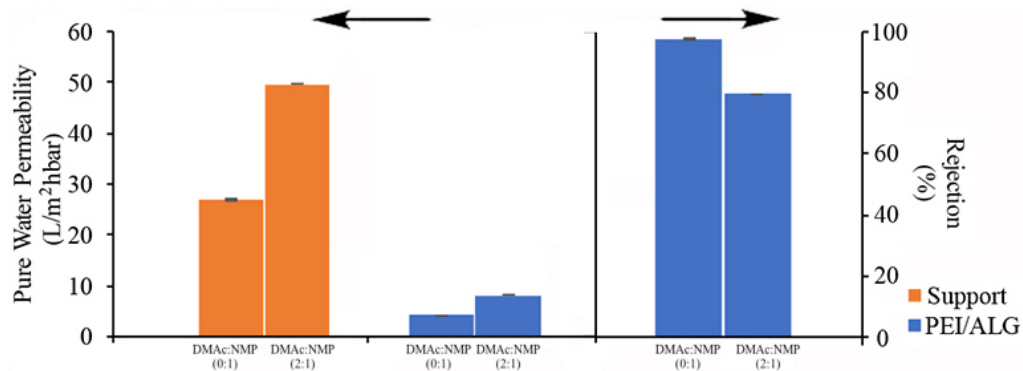


Figure 4.5. Effect of solvent type on membrane performance.

This result can be explained by the solubility parameter difference between polymer and solvent. As the difference between the solubility parameters of solvent and polymer becomes smaller, the interaction between those increases. Solubility parameter difference between PSF:SPES (5:1) and NMP is  $(4.35\text{MPa})^{0.5}$  higher than between PSF:SPES (5:1) and DMAC:NMP (2:1)  $(3.99\text{MPa})^{0.5}$  that results in a membrane with more aggregation of grains due to weaker interaction between solvent and polymer (Guan et al., 2005; Guillen et al. 2011). This might cause to obtain a less porous membrane. After one bilayer PEI/ALG coating, the permeability of this membrane was still higher but its PEG 1000 rejection was significantly lower than the corresponding values for the membrane prepared only with NMP.

Based on the results reported in this section, it was shown that the membrane in the NF category was manufactured. It was decided to continue casting the membranes with 25% polymer concentration (PSF:SPES blending ratio of 5) and 250 micron thickness. The PEG 6000 rejection of this membrane was determined as  $99.5\pm 0.45$  (MWCO < 6000 Da) and its cross section and surface SEM images are shown in Figure 4.6. The images have clearly shown that the support membrane has a finger-like structure (Figure 4.6 a) and its dense skin layer (Figure 4.6 b) is 2.3% of the total thickness. The pore size on the surface of the membrane (Figure 4.6 c) is much smaller than the bulk, measured around  $9.03\pm 0.88\text{ nm}$  using ImageJ software.



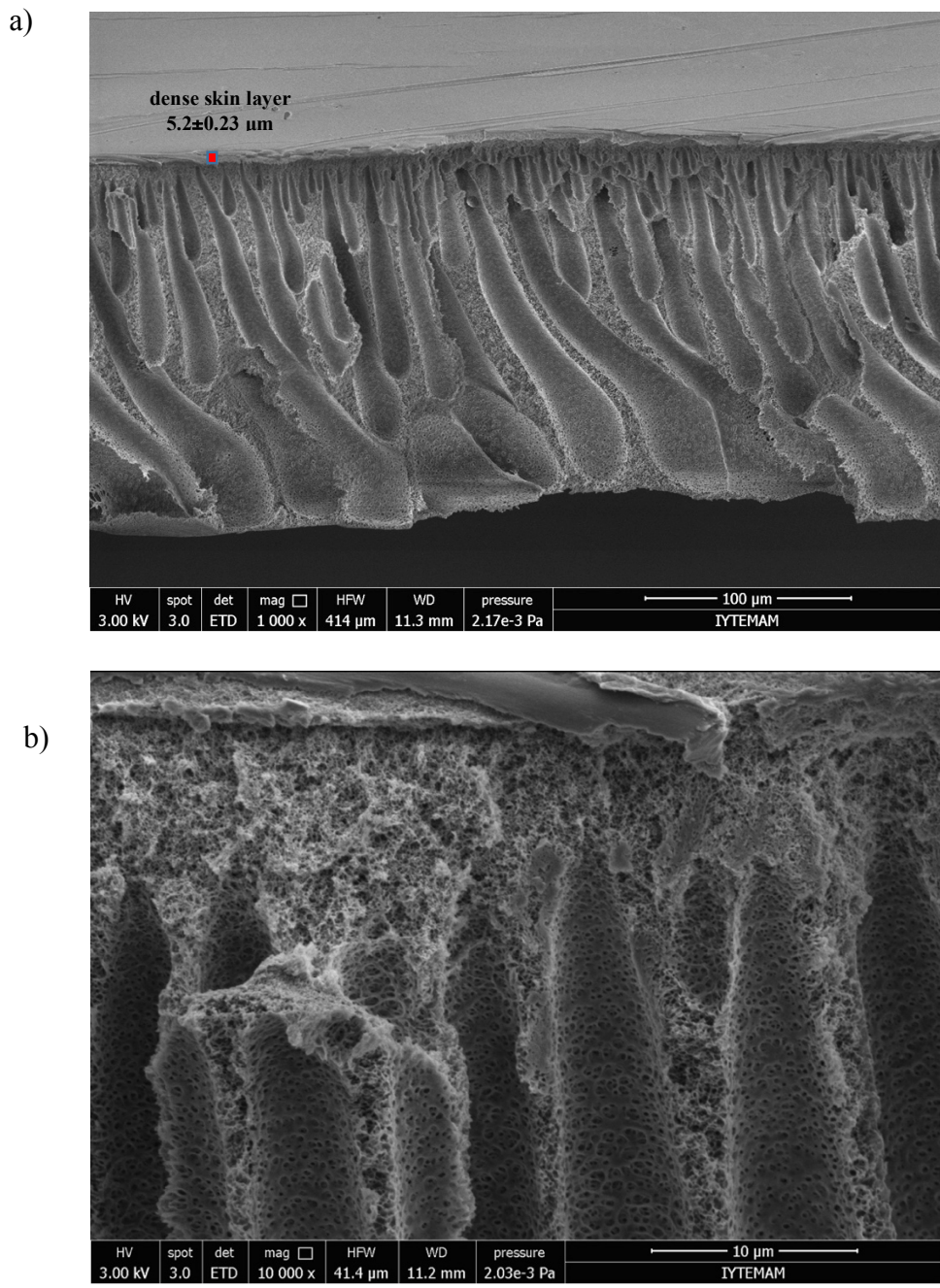


Figure 4.6. SEM images of the support membrane cast with 25 % polymer concentration (PSF:SPES blending ratio of 5) and 250 micron thickness. a) cross section, magnification 1000x b) cross section magnification 10000x c) surface magnification 100000x.

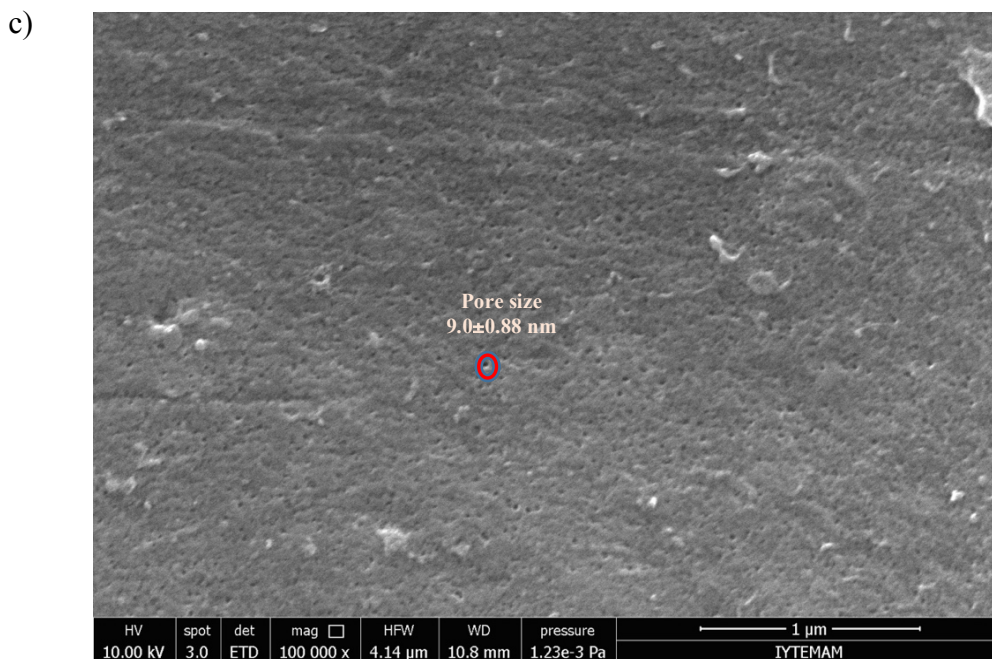


Figure 4.6. (cont.)

## 4.2. Optimization of Coating Conditions

After having decided support preparation conditions, the influences of the LbL coating conditions which are pH, concentration of supporting electrolyte, polyelectrolyte concentration and type of coating were investigated on the pure water permeability and PEG 1000 rejection of the TFC membranes prepared with PSF:SPES ratio of 5:1.

### 4.2.1. Optimization of Coating Conditions on Support Prepared with PSF:SPES Ratio of 5:1

#### 4.2.1.1. Effect of pH

Membrane performance is dramatically affected by the pH of weak polyelectrolyte deposition solutions since polymer charge density is a strong function of pH for weak polyelectrolytes (Joseph et al., 2014). In order to see the effect of pH on the membrane performance, the negatively charged support was first dynamically coated with 1 g/L of 750 kDa PEI solution in the presence of 0.5 M NaCl at pH 3 and 7

solutions at 1 bar. Single layer coating with PEI solution at pH 3 resulted in both higher pure water permeability (PWP) and PEG1000 rejection as shown in Figure 4.7.

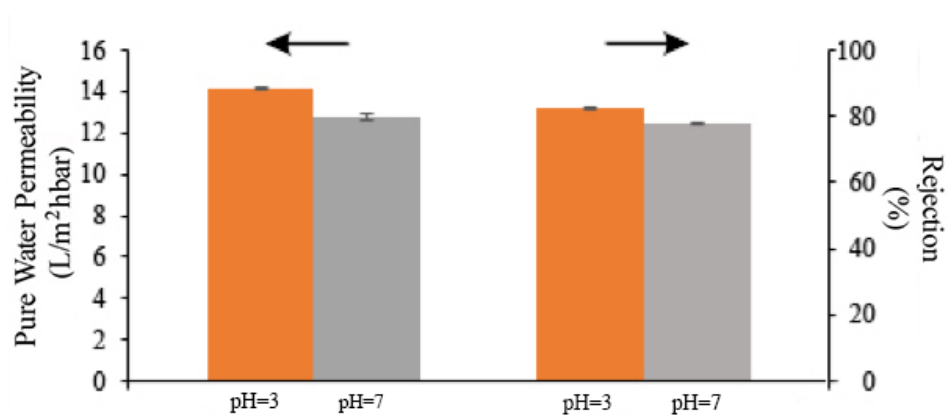


Figure 4.7. The effect of pH of PEI solution in the presence of 0.5 M NaCl on the membrane performance.

In order to understand the effect of pH on the surface property of the membranes, first both coated membranes were stained by congo red. Isoelectric point of congo red is around pH 3 and it carries more negative charge when its pH is increased (Yaneva and Georgieva, 2012). For staining 1 g/L of congo red solution at pH 7 was used and Figure 4.8 shows the color intensities measured on the membranes coated with PEI solution at pH 3 and 7. The results have shown that PEI-coated membrane at pH 7 resulted in higher intensity indicating that more congo red charged units interacted with PEI layer.

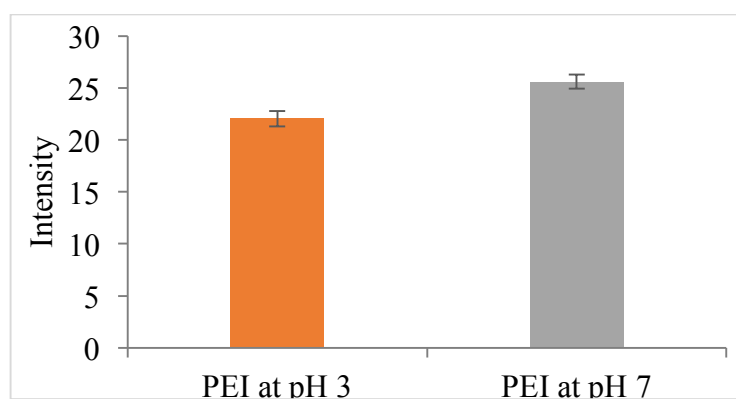


Figure 4.8. Intensity of PEI-deposited membranes at pH 3 and pH 7 in the presence of 0.5 M NaCl.

It was shown in the literature that PEI carries positive charge in a wide range of pH as represented in Table 4.6.

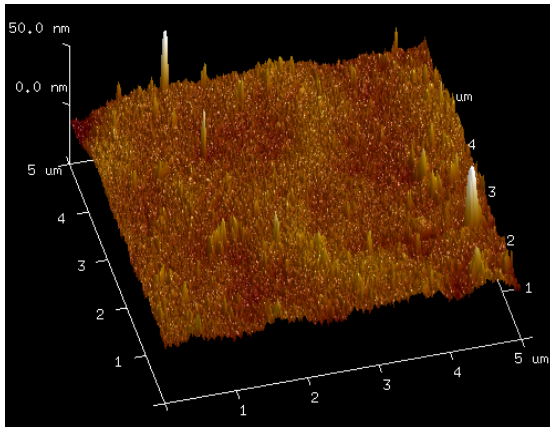
Table 4.6. Effect of pH on degree of protonation and Stokes-Einstein radius of 7200Da PEI.

Source: Adapted from (Lindquist and Stratton (1976))

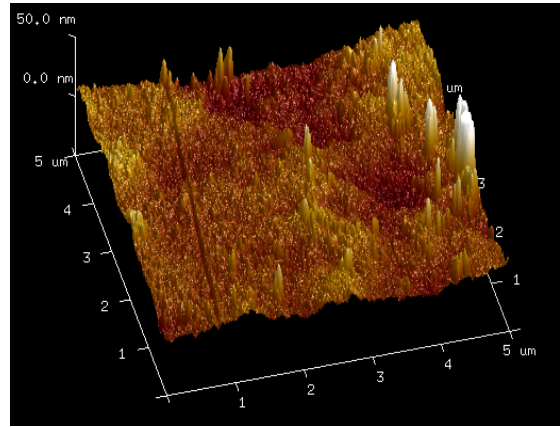
<b>pH</b>	<b>Degree of protonation (%)</b>	<b>Einstein-Stokes Diameter (nm)</b>
10.8	0	4.7
10.0	4	4.9
9	10	6.1
8	20	7.2
7	34	7.6
5	55	7.7
3	73	7.4

According to the data in Table 4.6, the degree of protonation of PEI at pH 3 is significantly higher than at pH 7, thus, it is expected that the membrane prepared with pH 3 carries more positive charge on the surface. Combining the data in Table 4.6 and the results in Figure 4.8, it can be concluded that higher color intensity measured for the membrane prepared with pH 7 PEI solution corresponds to more PEI adsorption at this pH. Otherwise, if the amount of PEI adsorbed at pH 3 and pH 7 was similar, then, an opposite result compared to the current data reported in Figure 4.8 should have been observed.

AFM images of PEI-coated membranes at pH 3 and 7 in the presence of 0.5 M NaCl were shown in Figure 4.9. At higher degree of ionization PEI corresponding to pH 3, the surface roughness was found lower.



a) RMS Roughness =  $2.72 \pm 0.16$  nm



b) RMS Roughness =  $4.1 \pm 0.34$  nm

Figure 4.9. AFM images of membranes deposited at a) pH=3 and b) pH=7 in the presence of 0.5 M NaCl.

This result is not surprising since highly charged polyelectrolytes are expected to produce thin, flat and compact surfaces in a rod-like configuration so as to minimize electrostatic energy. In contrary, less charged polymers are supposed to result in thick, rough and floppy films by adopting themselves in a coiled configuration (McAloney et al., 2001). Raposo et al. (2015) studied PAH/PAZO LbL films and demonstrated that poorly charged polyelectrolytes resulted in more rough surfaces. Choi et al. (2011) indicated that increment in roughness of deposited polyelectrolytes could be ascribed to the low charge density undergoing excessive deposition of components due to the diffusion of polymer chains into and out of the film.

From the filtration and characterization results, higher permeability at pH 3 could be ascribed to the less adsorbed PEI segments and thinner layer formation at higher degree of ionization, hence, lower resistance to flow. On the other hand, the reason for the higher PEG1000 rejection could be better surface coverage due to the flatter adsorption of PEI at low pH. Varga et al. (2011) studied the branched PEI coating on silica surface at different pH values and schematic representation of the adsorption process is shown in Figure 4.10. As shown in the scheme, when solution pH is increased from 4 to 6, the gap between surface and PEI segments increases enabling molecules to pass easily through those gaps despite increment in the adsorbed layer.

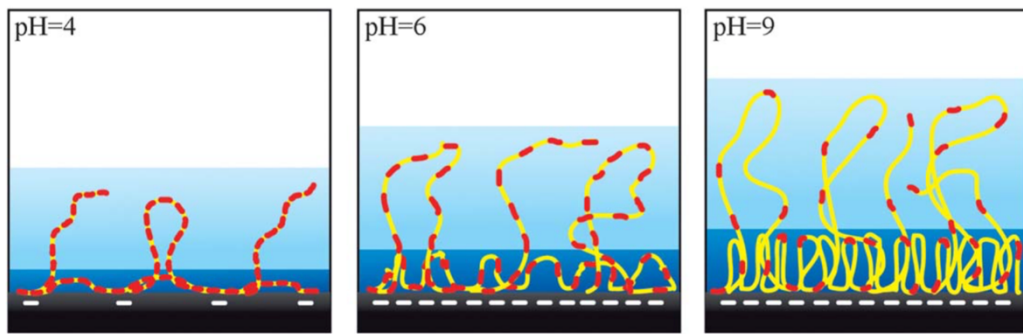


Figure 4.10. PEI layer adsorption at pH 4, 6 and 9.  
 (Source: Reprinted with permission from Varga et al. (2011))

In the demonstration, red lines represent positively charged segments whereas yellow segments denote uncharged portions. Silica support layer is shown as black region and deep and light blue correspond to inner and outer region of the adsorbed layer. From the figure, it is obvious that with the increment in pH lower degree of protonation of PEI results in more adsorption and higher thickness of adsorbed PEI segments (Varga et al., 2011).

Meszaros et al. (2002) demonstrated increased PEI adsorption with increased pH at fixed ionic strengths, since attractive surface/segment interactions gradually become dominant over the repulsive segment/segment interactions. On the other hand, at high segment charge density when pH is low, adsorption is low because of the strong segment/segment repulsion.

Hong et al. (2006) reported higher rejection and permeability of (PAA/PAH)<sub>4</sub>PAA membranes by obtaining more ionized structure as in the case reported here. They explained that thinner film is supposed to be obtained with highly ionized polyelectrolyte structure that suits the behavior represented in Figure 4.10. They observed that the film thickness decreased by 77% by depositing higher ionized polyelectrolytes. Choi and Rubner (2005) also indicated that if the weak polyelectrolyte begins to lose charge density, a dramatic increase in bilayer thickness occurs even over a very narrow pH range.

The effect of pH of PEI solution on the performance of one bilayer coated membrane was also examined. In both cases, the pH of the ALG solution coated on PEI layer was fixed at 7 and 0.5 M NaCl was added into PEI solution while ALG was dissolved in water without adding NaCl in it. According to the results shown in Figure 4.11, higher water permeability and lower PEG1000 rejection were obtained when ALG

solution was deposited on the surface covered by PEI at pH 3 compared to the corresponding values obtained when adsorbed on the pH 7 PEI modified support.

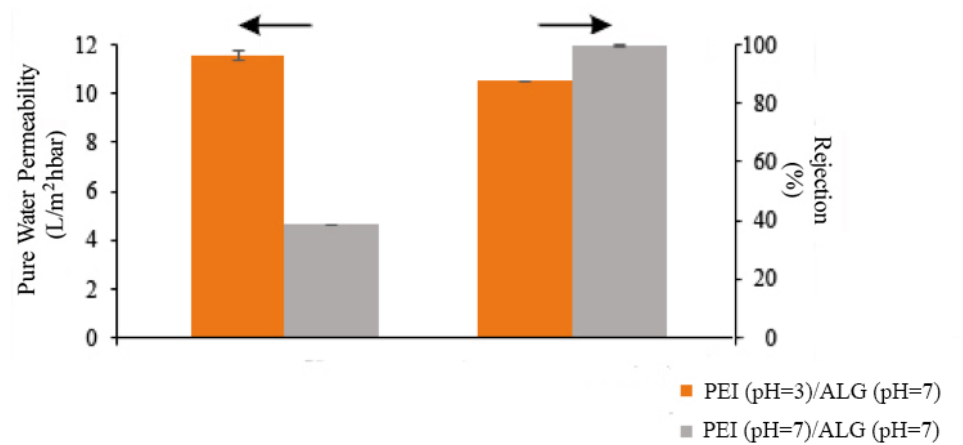


Figure 4.11. The effect of pH of PEI solution during PEI (0.5 M NaCl)/ ALG (0 M NaCl) deposition on the membrane performance.

This result can be explained by higher roughness of the surface modified with PEI at pH 7 which resulted in increment in surface area allowing more ALG adsorption (Schneider, 2015). In addition, higher amount of PEI deposition at pH 7 rather than pH 3 as shown in Figure 4.8 might facilitate more ALG adsorption owing to more electrostatic interaction.

Compared to one-layer PEI deposition at pH 3, PEG1000 rejection value increased from 82 % to 87 % while pure water permeability slightly decreased by successive coating of PEI and ALG.

#### 4.2.1.2. Effect of Supporting Electrolyte

The effect of adding 0.5 M NaCl into PEI solution at pH 3 and pH 7 was investigated. The results in Figure 4.12 and 4.13 have shown that at both pH 3 and 7 lower permeability and higher PEG 1000 rejection was obtained in the presence of salt.

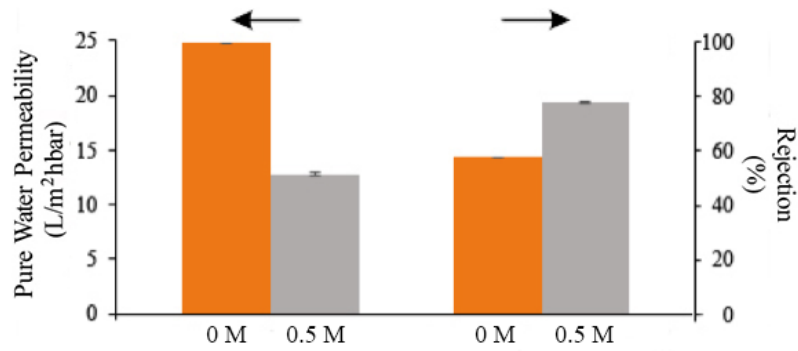


Figure 4.12. The effect of adding NaCl into PEI solution (pH=7) on the membrane performance.

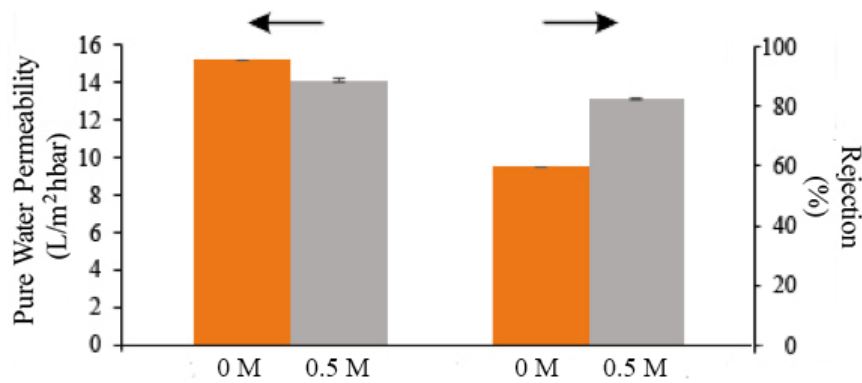


Figure 4.13. The effect of adding NaCl into PEI solution (pH=3) on the membrane performance.

At pH 7, water permeability decreased by 65 % and 29 % after dynamic coating of 750 kDa PEI in the presence and the absence of salt, respectively. On the other hand, in the case of pH 3, the decrease in pure water permeability after PEI coating in the presence and in the absence of salt was found similar (43 %). The advantage of using NaCl in the deposition solution was shown by higher PEG 1000 rejection (75 % at pH 7 and 82 % at pH 3) which means the membrane modified with the salt containing PEI solution is more suitable for NF applications. It was noted that the influence of ionic strength on the pure water permeability was more pronounced at pH 7 than at pH 3.

To investigate the relationship between ionic strength of the polyelectrolyte deposition solution and surface properties of the resulting membranes, staining experiments and AFM analysis were performed.



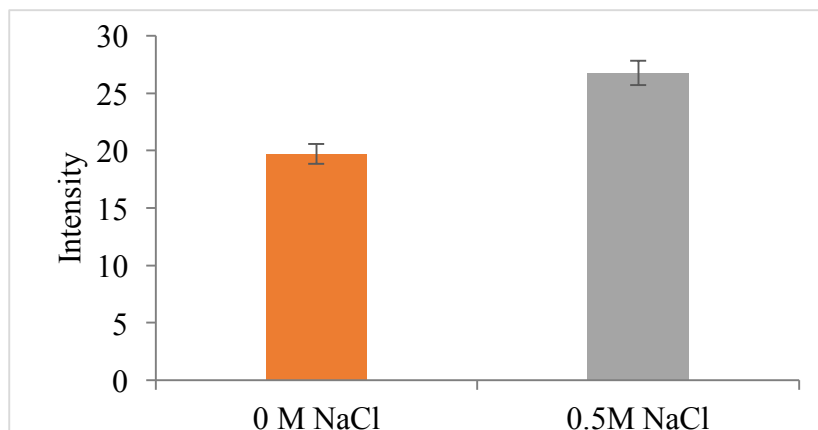


Figure 4.14. Intensity of PEI-deposited membranes in the absence and presence of 0.5 M NaCl at pH 7.

The results in Figure 4.14 have shown that in the presence of salt during deposition the charge density of the membrane becomes higher as confirmed by the higher color intensity measured on this membrane. The higher charge density might indicate higher PEI adsorption on the support membrane. Ouyang et al. (2008) also showed that polyelectrolyte solution with high ionic strength induced more charge near the surface and a larger amount of polyelectrolyte was adsorbed onto the oppositely charged membrane. Similarly, Meszaros et al. (2002) reported increased adsorption level for 750 kDa PEI when ionic strength was increased. This is due to the screening of segment/segment repulsion leading to attractive surface/segment interactions. On account of higher ionic strength, higher charge near the surface dominated the effects of increased charge screening.

From the AFM images shown in Figure 4.15, it was observed that the deposition of PEI with an ionic strength of 0 M either at pH 3 or pH 7 resulted in lower surface roughness as compared to the case in which salt was added into the polyelectrolyte solution. This result is consistent with the previous finding which reported that in the presence of high salt concentrations, PEI molecules are prone to become smaller and show aggregation tendency leading to an increase in the surface roughness (Kadioglu et al., 2010).

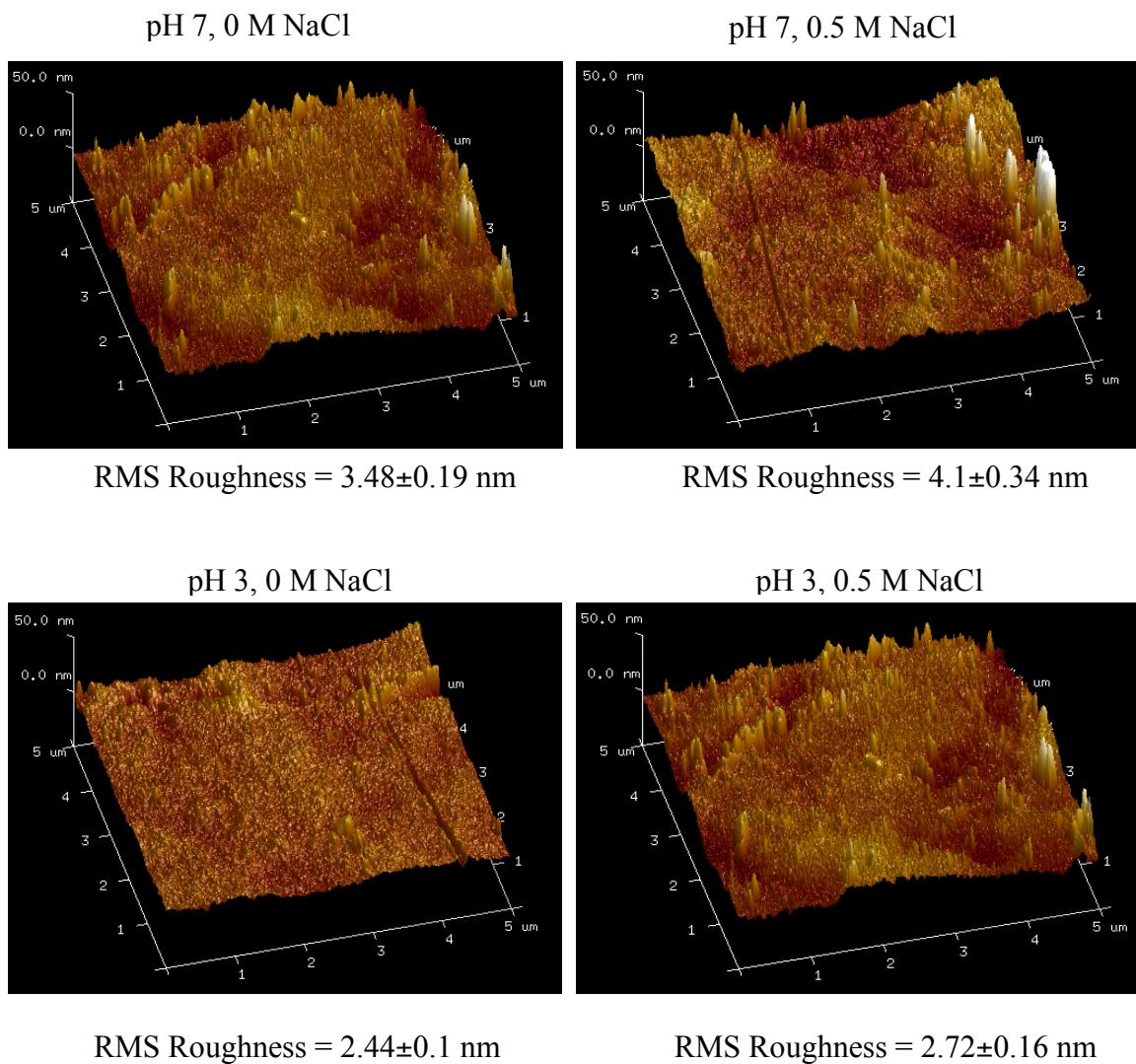


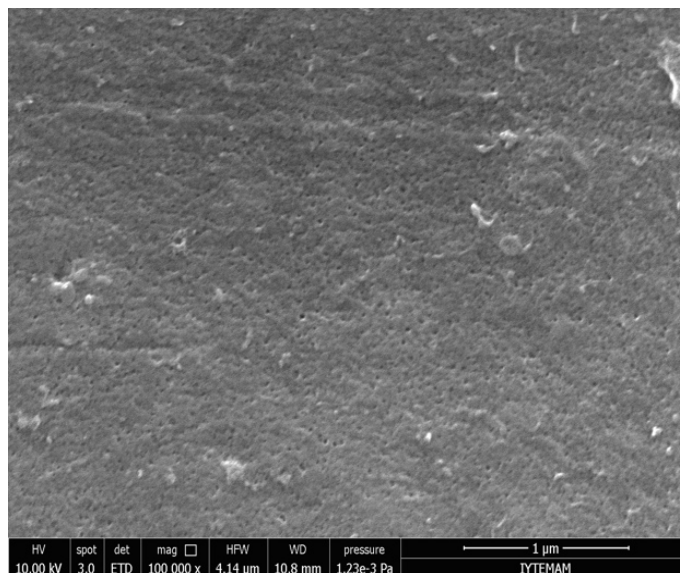
Figure 4.15. AFM images of the coated membranes.

Lower pure water permeability of PEI coated membrane at pH 7 in the presence of salt could be ascribed to the formation of thicker and more rough films as also reported in previous studies (McAloney et al., 2001; Ghostine et al., 2013). Higher color intensity on the membrane prepared in the presence of 0.5 M NaCl confirmed more PEI adsorption which resulted in higher PEG1000 rejection in comparison with PEI deposition at pH 7 without salt. Deposition of PEI solution at pH 3 in the presence or absence of supporting electrolyte did not change the pure water permeability since surface roughness of the deposited films was found similar (Figure 4.15). Higher PEG1000 retention in the presence of salt could be attributed to more polyelectrolyte adsorption as was also discussed by Meszaros et al. (2002).

From the figure 4.16, SEM images of support and coated membranes by PEI at pH 7 in the absence and presence of salt with same magnification were demonstrated. It

was obvious that, surface support had higher number of pores as compared to both coated case. On the other hand, membrane coated by PEI in the presence of salt seemed more rough in comparison with membrane in the absence of salt that overlapped with the data of AFM.

a)



b)

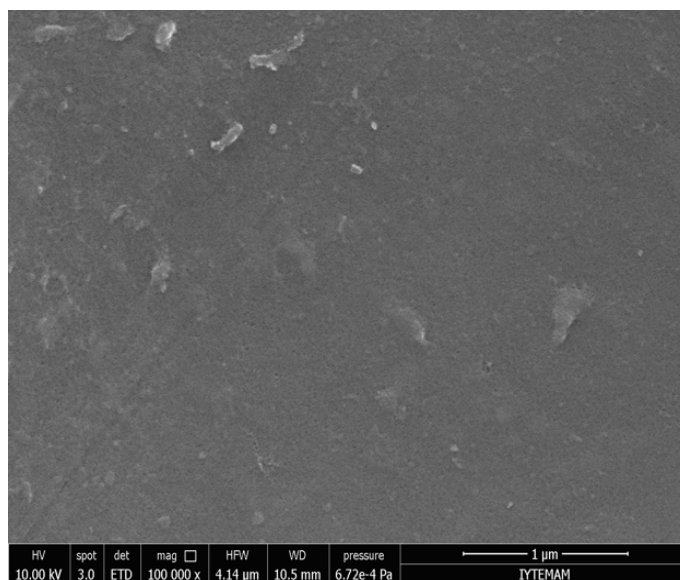


Figure 4.16. Surface SEM images of a) bare support and pH 7 PEI-coated membranes in the presence of b) 0 M NaCl c) 0.5 M NaCl.

c)

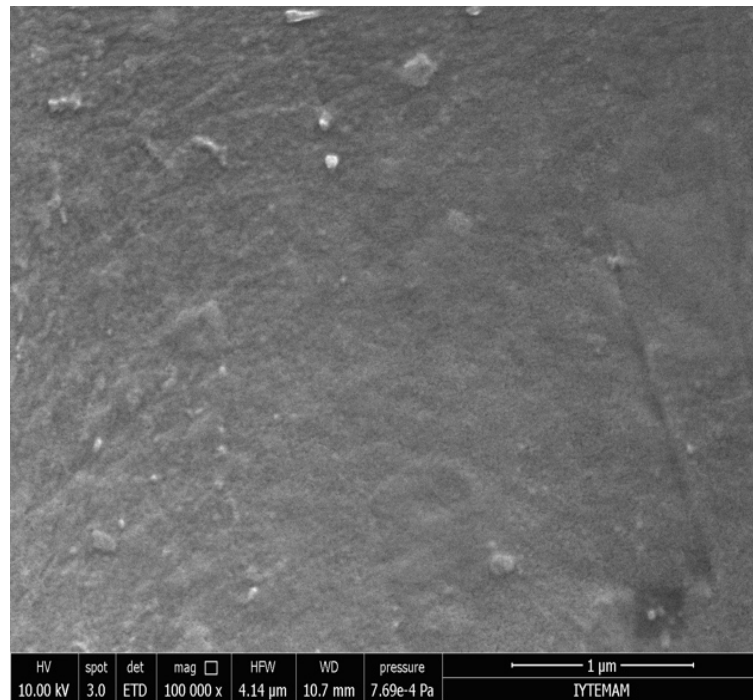


Figure 4.16. (cont.)

#### 4.2.1.3. Effect of Coating Type (Dynamic versus static)

The effect of coating type on the rejection and pure water permeability of the membranes was also investigated. For this purpose, the ALG layer was deposited under dynamic and static conditions onto the dynamically coated PEI layer. According to the results shown in Figure 4.17, higher permeability and lower rejection were obtained after static coating of ALG. This can be explained by the fact that in the case of dynamic coating, the polyelectrolyte solution was forced towards the membrane surface under pressure. Consequently, within the same time period, more ALG adsorption is expected covering the pores on the surface of the PEI layer compared to the static coating case in which ALG approaches to the surface by free diffusion.

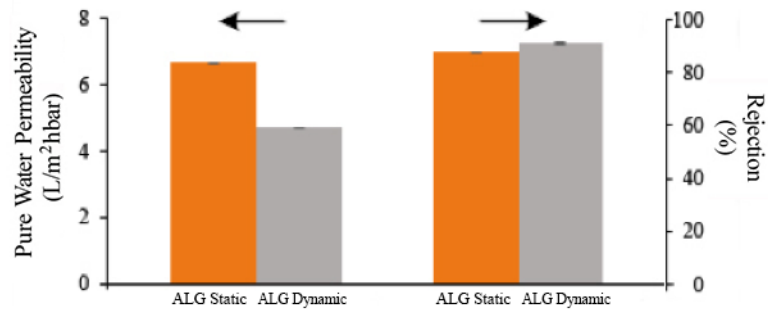


Figure 4.17. The effect of coating type on the membrane performance. NaCl concentrations in PEI (pH=7)/ALG (pH=7) solutions are 0.5 M and 0 M, respectively.

Menne et al. (2016) manufactured hollow fiber NF membrane by successive adsorption of polydiallyldimethylammonium chloride (PDADMAC) and polystyrene sulfonate (PSS) on polyethersulfone based UF support. They obtained higher water flux and better divalent rejection by replacing many statically adsorbed layers with just a few dynamically coated layers.

#### 4.2.1.4. Effect of Polyelectrolyte Concentration

To investigate the effect of polyelectrolyte concentration on the rejection and permeability, ALG with a concentration of 1 or 5 g/L was deposited statically on the PEI layer. The results have shown in Figure 4.18 that in order to reach the same rejection level of around 87 %, it was needed to increase the number of polyelectrolyte layers from 4 to 6 when ALG concentration was increased from 1 to 5 g/L. This occurs since at relatively high concentrations, polyelectrolyte segments prefer to interact with each other in the bulk phase rather than with the surface, as a result, more layers are needed to cover the surface. Using higher ALG concentration resulted in not only increased number of layers but also slightly lower permeability in order to reach same PEG 1000 rejection level (87%) as a result of increased mass transfer resistance to flow. Fler et al. (1993) observed that deposited layers were thicker when polyelectrolyte concentration was increased.

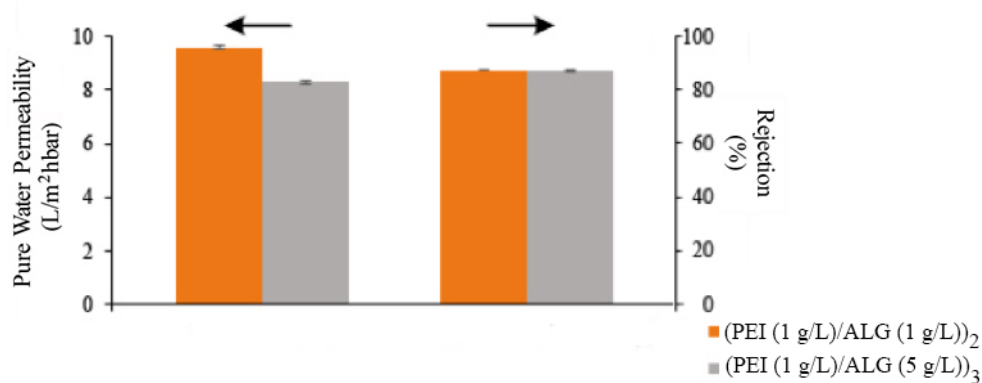


Figure 4.18. The effect of polyelectrolyte concentration on the membrane performance. NaCl concentrations in PEI(pH=7)/ALG(pH=7) solutions are 0.5 M and 0 M, respectively.

## 4.2.2. Optimization of Coating Conditions on Support Prepared with PSF:SPES Ratio 4:1

### 4.2.2.1. Effect of pH

Even though, preparation of TFC NF membrane with only bilayer deposition was demonstrated previously, further investigation was performed for the sake of improving pure water permeability of the produced NF membrane. For this purpose, PSF:SPES ratio in support membrane was changed from 5:1 to 4:1 to increase hydrophilic character of the resultant membrane in the presence of more SPES in the structure.

In the light of previous results obtained with the PSF:SPES ratio of 5:1, the two most significant parameters, pH and ionic strength of the polyelectrolyte solution, were investigated in the case of PSF:SPES ratio of 4:1. In the first case, the pH of the PEI solution was altered from 3 to 7 in the presence of 0.5 M NaCl, whereas pH of the ALG solution coated on PEI layer was fixed at 7 in the absence of NaCl in it. According to the results shown in Figure 4.19, higher water permeability and lower PEG1000 rejection were obtained when ALG was coated on the surface deposited by PEI at pH 3 rather than at pH 7.

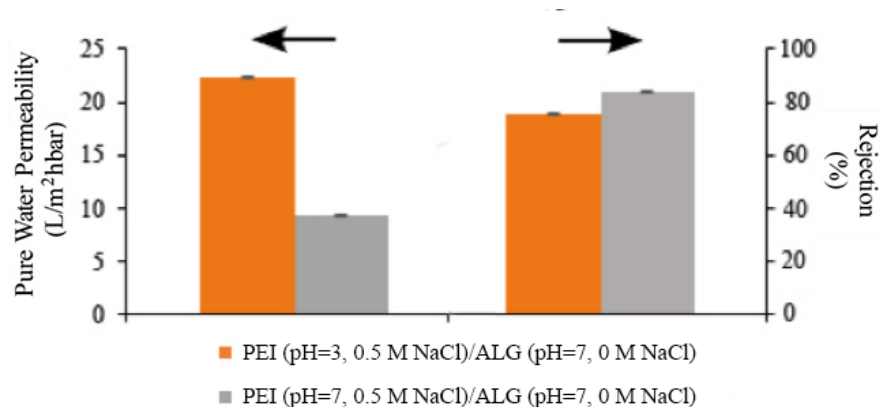


Figure 4.19. The effect of pH of PEI solution during PEI/ALG deposition on the membrane performance.

Compared to the results obtained with 5:1 PSF:SPES support, significant improvement was observed in the pure water permeability at the expense of lower PEG1000 rejection when the PSF:SPES ratio was decreased to 4:1. For example, when the pH of both polyelectrolytes were 7, pure water permeability increased from  $4.63 \pm 0.0$  to  $9.2 \pm 0.04$  L/m<sup>2</sup>.h.bar while PEG 1000 rejection decreased from  $99.6 \pm 0.2$  % to  $82.9 \pm 0.3$  %. This is an expected result since an increase in SPES composition in the blend membrane increases hydrophilicity and the increased molecular weight cut-off of the membrane was reported by Jacob et al. (2014). Figure 4.20 shows that the contact angle of the support membrane decreased from  $69.1 \pm 1.02$  to  $59.2 \pm 0.68$  when the PSF:SPES ratio changed from 5 to 4.



Figure 4.20. Contact angle measurement of support with PSF:SPES ratio a) 4:1 and b) 5:1.

When the pH of both polyelectrolytes was increased to 8 with 0.5 M NaCl only in PEI solution, the permeability and PEG 1000 rejection of resulting membrane were found as  $13.9$  L/m<sup>2</sup>.h.bar and 96 %, respectively.

Improved permeability and rejection of the membrane were attributed to high charge-charge interaction between ALG and PEI resulting in high degree of cross linking and smaller pores and thinner layer and lower resistance to flow. Both PEI and ALG carry highest charge density at pH 8 among pH 3, 7 and 8.

#### 4.2.2.2. Effect of Ionic Strength in ALG Layer

In Figure 4.21, ionic strength effect on both layers were investigated. When 0.5 M NaCl was added into the ALG layer, rejection was increased but flux was decreased. Ionic strength affected the ALG layer in the same way as in PEI layer and probably caused more adsorption of ALG to the PEI modified surface.

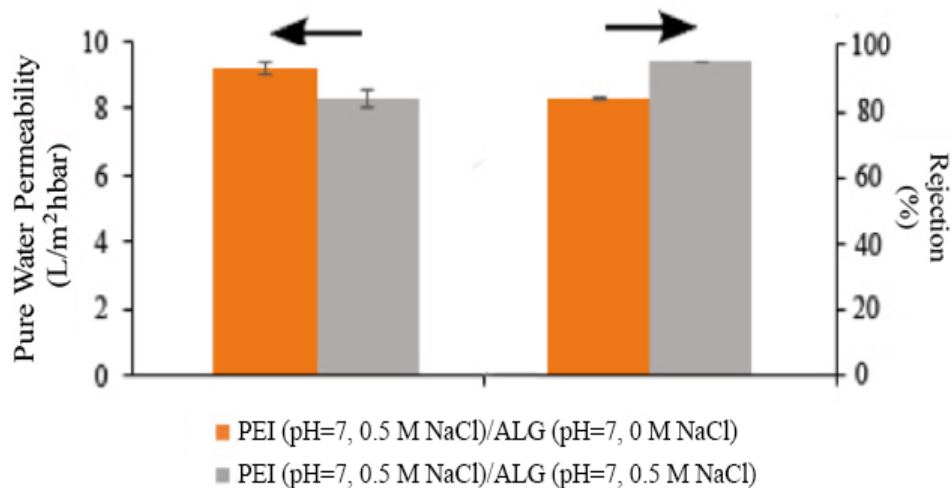


Figure 4.21. The effect of salt addition in ALG solution during PEI/ALG deposition on the membrane performance.

Cross section and surface SEM images of the membrane prepared with PSF:SPES ratio of 4 are shown in Figure 4.22. Dense skin layer of the support membrane is  $5.1 \pm 0.22 \mu\text{m}$  and the pore size on the surface of the membrane (Figure 4.6 c) was measured around  $9.86 \pm 0.16 \text{ nm}$  using ImageJ software.



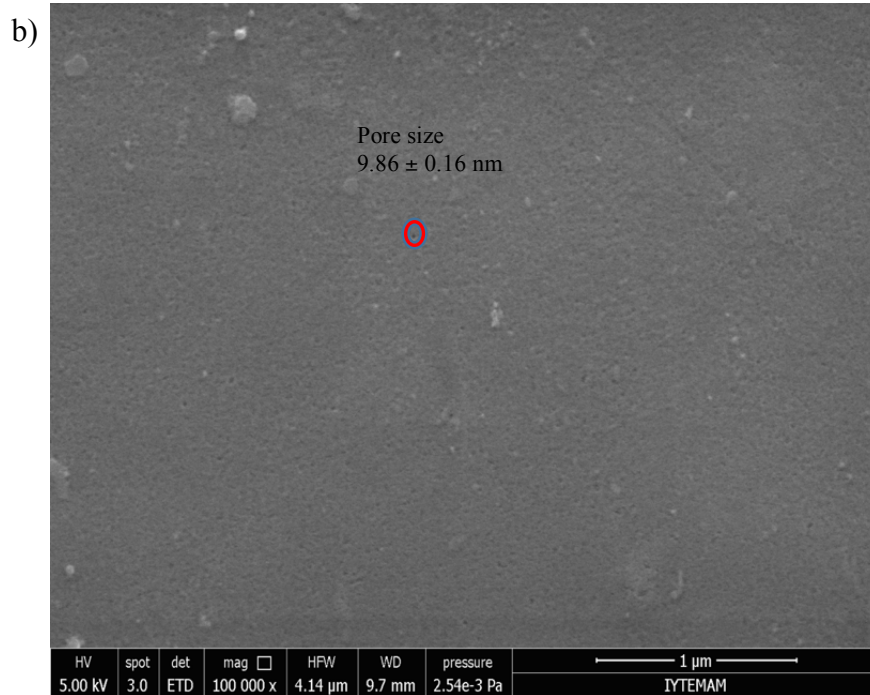
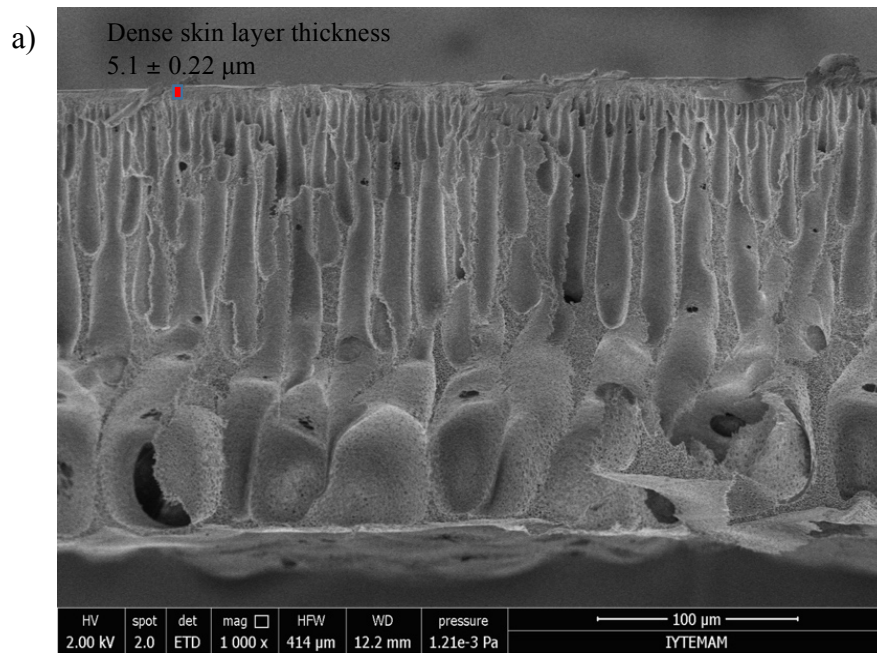


Figure 4.22. SEM images of the support membrane cast with 25 % polymer concentration (PSF:SPES blending ratio of 4) and 250 micron thickness. a) cross section magnification 1000x b) surface magnification, 100000x.

### 4.3. Fouling Tendency and Stability of the Membranes

#### 4.3.1. Antifouling property of LbL coated membrane

Fouling tendency of PEI/ALG coated membrane and commercial Sartorius polyethersulfone membrane were compared. Both membranes have a 1000 Da of MWCO. The fouling behaviour was investigated by filtering 1 g/L bovine serum albumin (BSA) in pure water at pH 7 since it is negatively charged at this pH. Figure 4.23 shows the dead-end filtration results in terms of normalized flux up to 15 h.

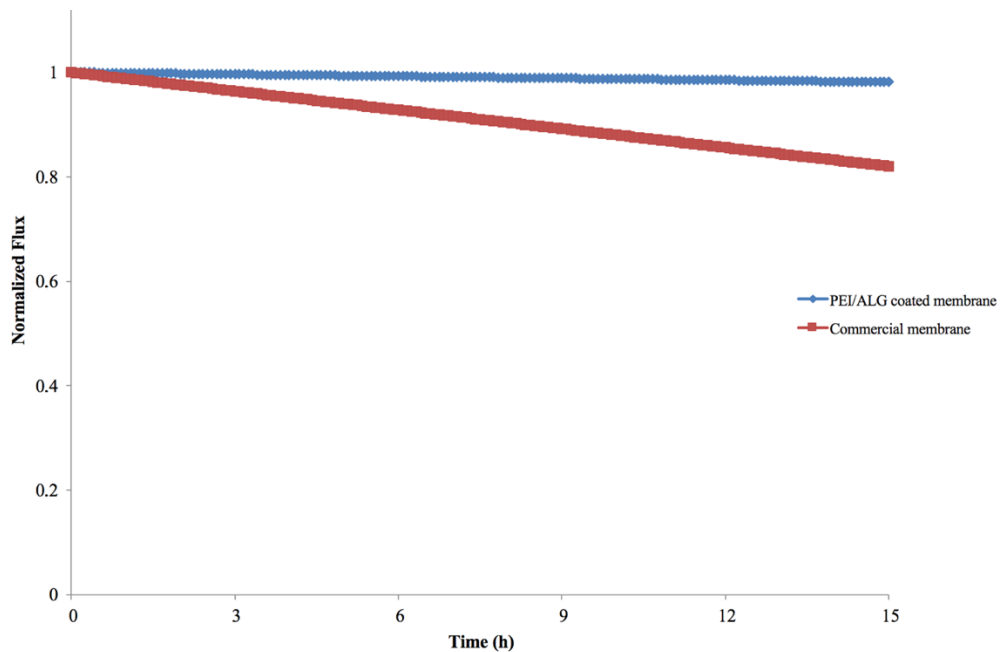


Figure 4.23. Fouling tendency of the produced NF membrane and commercial polyethersulfone membrane in dead-end filtration module.

Commercial polyethersulfone membrane showed flux decline around 20% over the course of the filtration, whereas PEI/ALG coated membrane produced in this study displayed almost constant flux performance during filtration, showed only 2 % flux decline. The outer surface of the membrane is negatively charged and rejects negatively charged BSA at pH 7. Better antifouling property of our membrane can be attributed to much more hydrophilic character of the surface. Pure water permeability of our membrane and commercial membrane are 13.9 and 1 L/m<sup>2</sup>hbar, respectively. Results in Table 4.7 shows that for both membranes most of the fouling due to accumulation of BSA is reversible and commercial membrane resistance is lower since it is a single

layer membrane. Due to more hydrophilic nature of the surface, recovery of flux after washing is higher in our membrane compared to the commercial one.

Table 4.7. Fouling resistances of the membranes.

	$R_{\text{membrane}}$ (%)	$R_{\text{reversible}}$ (%)	$R_{\text{irreversible}}$ (%)	$R_{\text{total}}$ (%)	Flux Recovery (%)
PEI/ALG Coated Membrane	81	12.5	6.5	100	92.5
Commercial Membrane	51.3	41.4	7.3	100	87.5

### 4.3.2. Stability of LbL coated layers

Stability of the PEI (pH=8, 0.5 M NaCl)/ALG (pH=8, 0 M NaCl) coated membrane was investigated by measuring pure water permeability and PEG1000 rejection after storing the membrane in 1 M NaCl solution up to 14 days.

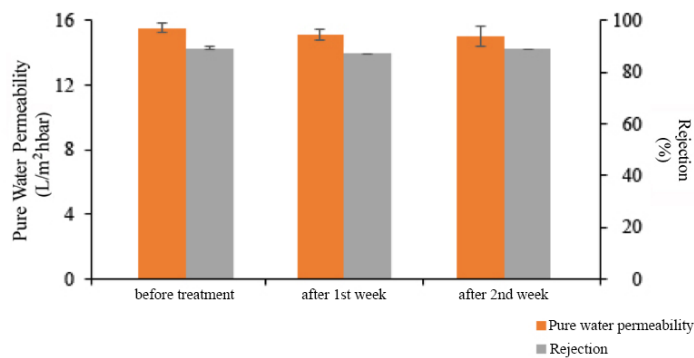


Figure 4.24. Stability measurement of PEI/ALG coated membrane.

Figure 4.24 demonstrates that performance of the membrane both in terms of rejection and pure water permeability stayed constant over 2 weeks of storage in 1 M NaCl. This result indicates that PEI and ALG layers are stable and do not detach from the surface under such a high NaCl concentration.

## CHAPTER 5

### CONCLUSION

In this thesis, NF membranes were prepared via LbL self-assembly of PEI/ALG bilayer on PSF/SPES support. In order to obtain NF membrane with only one bilayer of polyelectrolyte pair, the molecular weight cut off value for the support membrane should be less than 10 kDa. This was achieved by adjusting composition and thickness of casting solution as well as composition of the coagulation bath. The membranes were characterized in terms of their pure water permeabilities, PEG1000 rejection, organic fouling tendency and stabilities. In the case of single layer PEI deposition, adsorption at low pH values are suggested to achieve both high PEG 1000 rejection close to 90 % and pure water permeability not less than 10 L/m<sup>2</sup>.h.bar.

When the deposition pH of PEI solution is high, then, ALG layer should be coated on PEI to reach PEG 1000 rejection not less than 87%. By adjusting PSF:SPES ratio in support membrane and one bilayer deposition of PEI and ALG it is possible to obtain pure water permeability as high as 16 L/m<sup>2</sup>hbar and PEG 1000 rejection around 90%. Supporting electrolyte can be added into polyelectrolyte solution to improve rejection characteristics regardless of deposition pH. Moreover, many statically adsorbed layers can be replaced by dynamic coated few layers without altering membrane performance. The polyelectrolyte concentration affects the membrane performance and optimum concentration should be selected to fully cover the surface and to control the film thickness that has a significant role on membrane permeability. Produced TFC NF membrane showed resistance to high concentration NaCl solution. Fouling tendency of prepared membrane was measured relatively low. The membrane prepared in this study has a great potential to be used in pharmaceutical, food and biotechnology industry for recovering valuable neutral or charged low molecular weight compounds (< 1200 g/mole).

## REFERENCES

- Adusumilli, Maneesha. "Polyelectrolyte Multilayer Films for Ion Separation and Water." *Ph.D. Thesis*, Michigan State University, 2010.
- Ahmed, Sufyan Fadhil. "Preparation and Characterization of Hollow Fiber Nanofiltration Membranes." *Master's Thesis*, University of Technology, 2010.
- Ba, Chaoyi, David A. Ladner, and James Economy. "Using Polyelectrolyte Coatings to Improve Fouling Resistance of a Positively Charged Nanofiltration Membrane." *Journal of Membrane Science* 347, no. 1–2 (2010): 250–59.
- Bachok, Daeng Mohd Ashik. "Dye Removal By Thin Film Composite (TFC) Membrane Produced Through Interfacial Polymerization Technique." *Bachelor's Thesis*, Universiti Malaysia Pahang, 2012.
- Burke, S. E., and C. J. Barrett. "Controlling the Physicochemical Properties of Weak Polyelectrolyte Multilayer Films through Acid/base Equilibria." *Pure and Applied Chemistry* 76, no. 7–8 (2004): 1387–98.
- C. Alkire, Richar, Dieter M. Kolb, Jacek Lipkowski and Phil N. Ross. Chemically Modified Electrodes.
- Cheng, Shuying, Darren L. Oatley, Paul M. Williams, and Chris J. Wright. "Positively Charged Nanofiltration Membranes: Review of Current Fabrication Methods and Introduction of a Novel Approach." *Advances in Colloid and Interface Science* 164, no. 1–2 (2011): 12–20.
- Choi, Ikjun, Rattanon Suntivich, Felix A Plamper, Christopher V Synatschke, H E M Axel, and Vladimir V Tsukruk. "pH-Controlled Exponential and Linear Growing Modes of Layer-by-Layer Assemblies of Star Polyelectrolytes." *Journal of the American Chemical Society* 133, (2011): 9592–9606.
- Choi, Jeeyoung, and Michael F. Rubner. "Influence of the Degree of Ionization on Weak Polyelectrolyte Multilayer Assembly." *Macromolecules* 38, no. 1 (2005): 116–24.
- Curtis, Kimberly A., Danielle Miller, Paul Millard, Saswati Basu, Ferenc Horkay, and Preethi L. Chandran. "Unusual Salt and pH Induced Changes in Polyethylenimine Solutions." *PLOS ONE* 11, no. 9 (2016): 1–20.
- Dalwani, Mayur. "Thin Film Composite Nanofiltration Membranes for Extreme Conditions." *Ph.D. Thesis*, University of Twente, 2011.
- Escobar, Isabel C., and Bart Van Der Bruggen. "Microfiltration and Ultrafiltration Membrane Science and Technology." *Journal of Applied Polymer Science* 132, no. 21 (2015): 42042-61.

Fadhillah, F, S. M. J. Zaidi, Z. Khan, M. M. Khaled, F. Rahman, and P. T. Hammond. "Development of polyelectrolyte multilayer thin film composite membrane for water desalination application" *Desalination* 318, (2013): 19–24.

Fleer, G. J., M. A. Cohen Stuart, J. M. H. M. Scheutjens, T. Cosgrove, B. Vincent. *Polymers at Interfaces*. Chapman & Hall: Cambridge, U.K.: 1993.

Fu, Jinhong, Jian Ji, Liyan Shen, Alexander Ku, Axel Rosenhahn, Jiacong Shen, and Michael Grunze. "pH-Amplified Exponential Growth Multilayers : A Facile Method to Develop Hierarchical Micro- and Nanostructured Surfaces pH-Amplified Exponential Growth Multilayers : A Facile Method to Develop Hierarchical Micro- and Nanostructured Surfaces." *Society* 25, no. 8 (2009): 672–75.

Ghostine, Ramy A., Rana M. Jisr, Ali Lehaf, and Joseph B. Schlenoff. "Roughness and Salt Annealing in a Polyelectrolyte Multilayer." *Langmuir* 29, no. 37 (2013): 11742–50.

Guan, Rong, Hua Dai, Cuihua Li, Jianhong Liu, and Jing Xu. "Effect of Casting Solvent on the Morphology and Performance of Sulfonated Polyethersulfone Membranes." *Journal of Membrane Science* 277, no. 1–2 (2006.): 148–56.

Guillen, Gregory R., Yinjin Pan, Minghua Li, and Eric M V Hoek. "Preparation and Characterization of Membranes Formed by Nonsolvent Induced Phase Separation: A Review." *Industrial and Engineering Chemistry Research* 50, no. 7 (2011): 3798–3817.

Hobbs, Colin, Seungkwan Hong, and James Taylor. "Effect of Surface Roughness on Fouling of RO and NF Membranes during Filtration of a High Organic Surficial Groundwater." *Journal of Water Supply: Research and Technology - AQUA* 55, no. 7–8 (2006): 559–70.

Hong, Seong Uk, Ramamoorthy Malaisamy, and Merlin L. Bruening. "Optimization of Flux and Selectivity in  $\text{Cl}^-/\text{SO}_4^{2-}$  Separations with Multilayer Polyelectrolyte Membranes." *Journal of Membrane Science* 283, no. 1–2 (2006): 366–72.

Jacob, K. Noel, S. Senthil Kumar, A. Thanigaivelan, M. Tarun, and D. Mohan. "Sulfonated Polyethersulfone-Based Membranes for Metal Ion Removal via a Hybrid Process." *Journal of Materials Science* 49, no. 1 (2014): 114–22.

Jhaveri, Jainesh H., and Z. V. P. Murthy. "A Comprehensive Review on Anti-Fouling Nanocomposite Membranes for Pressure Driven Membrane Separation Processes." *Desalination* 379, (2016): 137–54.

Joseph, Nithya, Pejman Ahmadiannamini, Richard Hoogenboom, and Ivo. F. J. Vankelecom. "Layer-by-Layer Preparation of Polyelectrolyte Multilayer Membranes for Separation." *Polym. Chem.* 5, no. 6 (2014): 1817–1831.

Kadioglu, Sezin Islamoglu, Levent Yilmaz, Nihal Aydogan, and H. Onder Ozbelge. "Removal of Heavy Metals from Multicomponent Metal Mixtures by Polymer Enhanced Ultrafiltration: Effects of pH, Ionic Strength and Conformational Changes in Polymer Structure." *Separation Science and Technology* 45, no. 10 (2010): 1363–73.

Krasemann, Lutz, Ali Toutianoush, and Bernd Tieke. "Self-Assembled Polyelectrolyte Multilayer Membranes with Highly Improved Pervaporation Separation of Ethanol/water Mixtures." *Journal of Membrane Science* 18, no. 2 (2001): 221–228.

Lajimi, Ramzi Hadj, Ezdine Ferjani, Mohamed Sadok Roudesli, and André Deratani. "Effect of LbL Surface Modification on Characteristics and Performances of Cellulose Acetate Nanofiltration Membranes." *Desalination* 266, no. 1-3 (2011): 78-86.

Li, Yafei, Yanlei Su, Jianyu Li, Xueting Zhao, Runnan Zhang, Xiaochen Fan, Junao Zhu, Yanyan Ma, Yuan Liu, and Zhongyi Jiang. "Preparation of Thin Film Composite Nanofiltration Membrane with Improved Structural Stability through the Mediation of Polydopamine." *Journal of Membrane Science* 476, (2015): 10–19.

Lindquist, G M, and R A Stratton. 1976. "Role of Polyelectrolyte Charge-Density and Molecular-Weight on Adsorption and Flocculation of Colloidal Silica with Polyethylenimine." *Journal of Colloid and Interface Science* 55, no. 1 (1976): 45–59.

Liu, Guanqing, David M. Dotzauer, and Merlin L. Bruening. "Ion-Exchange Membranes Prepared Using Layer-by-Layer Polyelectrolyte Deposition." *Journal of Membrane Science* 354, no. 1–2 (2010): 198–205.

Loosli, Frédéric, Philippe Le Coustumer, and Serge Stoll. "Effect of Natural Organic Matter on the Disagglomeration of Manufactured TiO<sub>2</sub> Nanoparticles." *Environmental Science: Nano* 1, no. 2 (2014): 154-160.

Malaisamy, Ramamoorthy, and Merlin L. Bruening. "High-Flux Nanofiltration Membranes Prepared by Adsorption of Multilayer Polyelectrolyte Membranes on Polymeric Supports." *Langmuir* 21, no. 23 (2005): 10587–10592.

McAloney, Richard A., Mark Sinyor, Vyacheslav Dudnik, and M. Cynthia Goh. "Atomic Force Microscopy Studies of Salt Effects on Polyelectrolyte Multilayer Film Morphology." *Langmuir* 17, no. 21 (2001): 6655–63.

Menne, Daniel, Johannes Kamp, John Erik Wong, and Matthias Wessling. "Precise Tuning of Salt Retention of Backwashable Polyelectrolyte Multilayer Hollow Fiber Nanofiltration Membranes." *Journal of Membrane Science* 499, (2016): 396–405.

Meszaros, Robert, Laurie Thompson, Martin Bos, and Peter de Groot. "Adsorption and Electrokinetic Properties of Polyethylenimine on Silica Surfaces," *Langmuir* 18, no. 13 (2002): 6164–69.

Michel, Marc, Valérie Toniazzo, David Ruch, and Vincent Ball. "Deposition Mechanisms in Layer-by-Layer or Step-by-Step Deposition Methods: From Elastic and Impermeable Films to Soft Membranes with Ion Exchange Properties." *ISRN Materials Science* 2012, (2012): 1–13.

Minhas, Fozia T., Shahabuddin Memon, M. I. Bhangar, Nadeem Iqbal, and M. Mujahid. "Solvent Resistant Thin Film Composite Nanofiltration Membrane: Characterization and Permeation Study." *Applied Surface Science* 282, (2013): 887–97.

Mulder, Marcel. *Basic Principles of Membrane Technology*. Kluwer Academic Publisher: 1996.

Ng, Law Yong, Abdul Wahab Mohammad, and Ching Yin Ng. "A Review on Nanofiltration Membrane Fabrication and Modification Using Polyelectrolytes: Effective Ways to Develop Membrane Selective Barriers and Rejection Capability." *Advances in Colloid and Interface Science* 197–198, (2013): 85-107.

Ning, Robert Y. "Phase Diagram and Membrane Desalination." *Desalination Updates*.

Ouyang, Lu, Ramamoorthy Malaisamy, and Merlin L. Bruening. "Multilayer Polyelectrolyte Films as Nanofiltration Membranes for Separating Monovalent and Divalent Cations." *Journal of Membrane Science* 310, no. 1–2 (2008): 76–84.

Pendergast, MaryTheresa M., and Eric M.V. Hoek. "A Review of Water Treatment Membrane Nanotechnologies." *Energy & Environmental Science* 4, no. 6 (2011): 1946-1971.

Qin, Zhenping, Changle Geng, Hongxia Guo, Ziang Du, Guojun Zhang, and Shulan Ji. "Synthesis of Positively Charged Polyelectrolyte Multilayer Membranes for Removal of Divalent Metal Ions." *Journal of Materials Research* 28, no. 11 (2013): 1449–57.

Rajabzadeh, Saeid, Chang Liu, Lei Shi, and Rong Wang. "Preparation of Low-Pressure Water Softening Hollow Fiber Membranes by Polyelectrolyte Deposition with Two Bilayers." *Desalination* 344, (2014): 64–70.

Rajesh, S., S. Senthilkumar, A. Jayalakshmi, M. T. Nirmala, A. F. Ismail, and D. Mohan. "Preparation and Performance Evaluation of Poly (Amide-Imide) and TiO<sub>2</sub> Nanoparticles Impregnated Polysulfone Nanofiltration Membranes in the Removal of Humic Substances." *Colloids and Surfaces A: Physicochemical and Engineering Aspects* 418, (2013): 92–104.

Raposo, Maria, Quirina Ferreira, Ana Rita, Monteiro Timóteo, Paulo A Ribeiro, Ana Maria, Paulo A. Ribeiro and Ana Maria Botelho do Rego. "Contribution of Counterions and Degree of Ionization for Birefringence Creation and Relaxation Kinetics Parameters of PAH / PAZO Films" *Journal of Applied Physics* 118, (2015): 114504-12.

Saeki, Daisuke, Masaaki Imanishi, Yoshikage Ohmukai, Tatsuo Maruyama, and Hideto Matsuyama. "Stabilization of Layer-by-Layer Assembled Nanofiltration Membranes by Crosslinking via Amide Bond Formation and Siloxane Bond Formation." *Journal of Membrane Science* 447, (2013): 128–33.

Sanyal, Oishi, and Ilsoon Lee. "Recent Progress in the Applications of Layer-By-Layer Assembly to the Preparation of Nanostructured Ion-Rejecting Water Purification Membranes." *Journal of Nanoscience and Nanotechnology* 14, no. 3 (2014): 2178–89.

Sanyal, Oishi. "Design of Polyelectrolyte Multilayer Membranes for Ion Rejection and Wastewater Effluent Treatment." *Ph.D.Thesis*, Michigan State University, 2016.



Schäfer, Andrea I., Nikolaos Andritsos, Anastasios J. Karabelas, Eric M. V. Hoek, René Schneider, and Marianne Nyström. "Fouling in Nanofiltration." *Nanofiltration - Principles and Applications*. Elsevier, 169-239, 2004.

Schneider, Hans-Jorg. *Chemoresponsive Materials: Stimulation by Chemical and Biological Signals*, 2015. <http://dx.doi.org/10.1039/9781782622420>

Stanton, Brian W., Jeremy J. Harris, Matthew D. Miller, and Merlin L. Bruening. "Ultrathin, Multilayered Polyelectrolyte Films as Nanofiltration Membranes." *Langmuir* 19, (2003),7038–42.

SU, Baowei, Tingting Wang, Zongwen Wang, Xueli Gao, and Congjie Gao. "Preparation and Performance of Dynamic Layer-by-Layer PDADMAC/PSS Nanofiltration Membrane." *Journal of Membrane Science* 423–424, (2012): 324–31.

Sun, Jingjing. "Layer-by-Layer Self-Assembly of Nanofiltration Membrane for Water and Wastewater Treatment." *Master's thesis*, University of Waterloo, 2015.

Varga, Imre, Amália Mezei, Róbert Mészáros, and Per M. Claesson. "Controlling the interaction of poly(ethylene imine) adsorption layers with oppositely charged surfactant by tuning the structure of the preadsorbed polyelectrolyte layer." *Soft Matter* 7, no. 22 (2011): 10701-10712.

Wang, Jinwen, Yaxuan Yao, Zhongren Yue, and James Economy. "Preparation of Polyelectrolyte Multilayer Films Consisting of Sulfonated Poly (Ether Ether Ketone) Alternating with Selected Anionic Layers." *Journal of Membrane Science* 337, no. 1–2 (2009): 200–207.

Wang, Kai Yu, and Tai Shung Chung. "The Characterization of Flat Composite Nanofiltration Membranes and Their Applications in the Separation of Cephalexin." *Journal of Membrane Science* 247, no. 1–2 (2005): 37–50.

Wu, Peng and Masanoa Imani. "Novel Biopolymer Composite Membrane Involved with Selective Mass Transfer and Excellent Water Permeability." *Advancing Desalination*. Intech: 2012.

Xu, Jia, Xianshe Feng, and Congjie Gao. "Surface Modification of Thin-Film-Composite Polyamide Membranes for Improved Reverse Osmosis Performance." *Journal of Membrane Science* 370, no. 1–2 (2011): 116–23.

Yaneva, Z., and N. Georgieva. "Insights into Congo Red Adsorption on Agro-Industrial Materials - Spectral, Equilibrium, Kinetic, Thermodynamic, Dynamic and Desorption Studies. A Review." *International Review of Chemical Engineering* 4, (2012): 127–46.

Yun, Hyung-joong, Hyobong Hong, Jouhahn Lee, and Chel-jong Choi. "Chemical and Structural Properties of Polyethyleneimine Film Coated on a SiO<sub>2</sub> Substrate in Different Concentrations." *Materials Transactions* 55, no. 5 (2014): 801-805.

Zhao, Qiang, Quanfu F. An, Yanli Ji, Jinwen Qian, and Congjie Gao. "Polyelectrolyte Complex Membranes for Pervaporation , Nanofiltration and Fuel Cell Applications." *Journal of Membrane Science* 379, no: 1-2 (2011): 19–45.

Zhou, Guichen, Ying Lu, He Zhang, Yan Chen, Yuan Yu, Jing Gao, Duxin Sun, Guoqing Zhang, Hao Zou, and Yanqiang Zhong. "A Novel Pulsed Drug-Delivery System: Polyelectrolyte Layer-by-Layer Coating of Chitosan-Alginate Microgels." *International Journal of Nanomedicine* 8, (2013): 877–87.